Vaccine-induced protection from homologous Tier 2 simian-human immunodeficiency virus challenge in nonhuman primates

AUTHORS: Matthias G. Pauthner[1,2,3,†], Joseph P. Nkolola[4,†], Colin Havenar-Daughton[2,5,‡], Ben Murrell[6,‡], Samantha M. Reiss[2,5,‡], Raiza Bastidas[1,2,3], Jérémie Prévost[7,8], Rebecca Nedellec[1,2,3], Benjamin von Bredow[9], Peter Abbink[4], Christopher A. Cottrell[2,3,10], Daniel W. Kulp[11], Talar Tokatlian[2,12], Bartek Nogal[2,3,10], Matteo Bianchi[1,2,3], Hui Li[13], Jeong Hyun Lee[2,5], Salvatore T. Butera[1,2], David T. Evans[9], Lars Hangartner[1,2,3], Andrés Finzi[7,8,14], Ian A. Wilson[2,3,10], Rich T. Wyatt[1,2,3], Darrell J. Irvine[2,12,15,16,17], William R. Schief[1,2,3], Andrew B. Ward[2,3,10], Rogier W. Sanders[18,19], Shane Crotty[2,5,6,*], George M. Shaw[13,*], Dan H. Barouch[4,15,†,*], Dennis R. Burton[1,2,3,15,†,*,#]

AFFILIATIONS/FOOTNOTES:

[1]Department of Immunology and Microbiology, The Scripps Research Institute, La Jolla, CA 92037, USA;

[2]Center for HIV/AIDS Vaccine Immunology and Immunogen Discovery (CHAVI-ID), The Scripps Research Institute, La Jolla, CA 92037, USA;

[3]IAVI Neutralizing Antibody Center and the Collaboration for AIDS Vaccine Discovery (CAVD), The Scripps Research Institute, La Jolla, CA 92037, USA;

[4]Center for Virology and Vaccine Research, Beth Israel Deaconess Medical Center, Harvard Medical School, Boston, MA 02215, USA;

[5]Division of Vaccine Discovery, La Jolla Institute for Allergy and Immunology, La Jolla, CA 92037, USA;

[6]Division of Infectious Diseases, Department of Medicine, University of California San Diego, La Jolla, CA 92037, USA;

[7]Centre de Recherche du CHUM, Montreal, QC, H2X 0A9, Canada

[8]Department of Microbiology, Infectious Diseases and Immunology, Université de Montréal, Montreal, QC, H2X 0A9, Canada

[9]Department of Pathology and Laboratory Medicine, University of Wisconsin-Madison, Madison, WI 53705, USA;

[10]Department of Integrative Structural and Computational Biology and the Skaggs Institute for Chemical Biology, The Scripps Research Institute, La Jolla, CA 92037, USA;

[11]Vaccine and Immunotherapy Center, The Wistar Institute, Philadelphia, PA 19104, USA;

[12]Koch Institute for Integrative Cancer Research, MIT, Cambridge, MA 02139, USA;

[13]Department of Medicine, University of Pennsylvania, Philadelphia, PA 19104, USA;

[14]Department of Microbiology and Immunology, McGill University, Montreal, QC, H3A 2B4, Canada

[15]Ragon Institute of Massachusetts General Hospital, Massachusetts Institute of Technology, and Harvard University, Cambridge, MA 02139, USA;

[16]Howard Hughes Medical Institute, Chevy Chase, MD 20815, USA;

[17]Departments of Biological Engineering and Materials Science & Engineering, MIT, Cambridge, MA 02139, USA;

[18]Department of Medical Microbiology, Academic Medical Center, University of Amsterdam, 1105 AZ Amsterdam, the Netherlands;

[19]Department of Microbiology and Immunology, Weill Medical College of Cornell University, New York, NY 10065, USA;

†These authors contributed equally to the work

‡Co-second authors

*Corresponding author: shane@lji.org, shawg@pennmedicine.upenn.edu, dbarouch@bidmc.harvard.edu, burton@scripps.edu

#Lead contact: burton@scripps.edu

55 **SUMMARY:**

56 Passive administration of HIV neutralizing antibodies (nAbs) can protect macaques from
57 hard-to-neutralize (Tier 2) chimeric simian-human immunodeficiency virus (SHIV)
58 challenge. However, conditions for nAb-mediated protection following vaccination have
59 not been established. Here, we selected groups of 6 rhesus macaques with either high
60 or low serum nAb titers from a total of 78 animals immunized with recombinant native-like
61 (SOSIP) Env trimers from the BG505 HIV isolate. Repeat intrarectal challenge with
62 homologous Tier 2 $SHIV_{BG505}$ led to rapid infection in unimmunized and low-titer animals.
63 In contrast, high-titer animals demonstrated protection that was gradually lost as nAb
64 titers waned over weeks to months. From these results, we determined that an autologous
65 serum ID_{50} nAb titer of ~1:500 was required to afford over 90% protection from medium-
66 dose SHIV infection. We further identified autologous nAb titers, but not ADCC or T cell
67 activity, as strong correlates of protection. These results provide proof-of-concept that
68 Env protein-based vaccination strategies can protect against hard-to-neutralize SHIV
69 challenge in rhesus macaques by inducing Tier 2 nAbs, provided appropriate neutralizing
70 titers can be reached and maintained.

71

72 **KEYWORDS:**

73 HIV vaccine, neutralizing antibodies, BG505, Tier 2 protection, non-human primates,
74 ADCC

INTRODUCTION:

Several vaccine strategies are being pursued to stimulate protective immunity against HIV, including those that combine the elicitation of cellular and humoral responses (Haynes and Burton, 2017; Stephenson et al., 2016). One of the most intensively studied approaches is focused on inducing neutralizing antibodies (nAbs) to the virus. Early pioneering monkey studies showed that DNA/gp120-immunization induces nAb responses that can protect against Tier 1 virus challenge (Barnett et al., 2008; 2010; Pal et al., 2006). However, Tier 1 viruses like $SHIV_{Ba\text{-}L}$ and $SHIV_{SF162\text{-}P4}$ are easy to neutralize, typically lead to self-limiting infections and are not considered representative of circulating viruses in the HIV pandemic. Two recent studies investigated vaccine-induced protection from a mixed Tier SIVsmE660 swarm and attributed protection, in part, to nAb and other Ab responses (Keele et al., 2017; Roederer et al., 2015). Currently there has not been clear evidence of vaccination-induced nAbs providing protection against viruses possessing hard-to-neutralize clinically relevant Tier 2 HIV Env in humans or NHP models.

Enthusiasm for the nAb approach arises from the association of nAbs with protection for other viruses (Tomaras and Plotkin, 2017) and the demonstration that passively administered HIV-neutralizing monoclonal antibodies (mAbs) can afford protection in monkey and mouse models of HIV infection (Gautam et al., 2016; Gruell et al., 2013; Hessell et al., 2007; Mascola et al., 2000; Moldt et al., 2012; Parren et al., 2001; Pegu et al., 2014; Shingai et al., 2014). As HIV does not infect monkeys, HIV-neutralizing mAbs are assessed by their ability to protect against chimeric simian-human immunodeficiency virus (SHIV) challenge in rhesus macaques (*Macaca mulatta*).

However, a major problem in establishing vaccine-induced nAb protection in the SHIV/macaque model has been the notorious difficulty in inducing nAbs by immunization. Indeed, induction of broadly neutralizing antibodies (bnAbs) via immunization has thus far only been achieved reproducibly in cows (Sok et al., 2017). However, we recently showed reliable induction of autologous strain-specific nAbs in macaques against a hard-to-neutralize Tier 2 HIV isolate through use of well-ordered and stabilized HIV envelope glycoprotein (Env) SOSIP trimers as immunogens in optimized approaches (Pauthner et al., 2017), building on previous SOSIP immunization studies in NHPs (Havenar-Daughton et al., 2016; Sanders et al., 2015; Torrents de la Peña et al., 2017). To carry out a protection experiment in macaques then requires construction of a SHIV with the same Env sequence as the immunizing trimer. Fortunately, it has recently become possible to reliably generate infectious SHIVs using *env* sequences from most primary Tier 2 HIV strains (Del Prete et al., 2017; Li et al., 2016).

In this study, building upon the advances in both trimer-based immunization strategies and SHIV generation, we immunized macaques with SOSIP trimers of the BG505 *env* sequence (de Taeye et al., 2015; Kulp et al., 2017; Torrents de la Peña et al., 2017), induced BG505-specific Tier 2 nAbs, and then challenged animals intrarectally with the neutralization-resistant, pathogenic $SHIV_{BG505}$ (Li et al., 2016), that carries the S375Y mutation to increase infectivity in NHPs. We found that protection could be achieved and was critically dependent on the level of serum nAb titers, but not on other antibody parameters such as V3 binding titers, antibody-dependent cellular cytotoxicity (ADCC), or the induction of T cell activity. We determined an approximate threshold titer

120 for vaccine-induced protection that establishes an experimental benchmark for
121 comparison with nAb-based vaccines to HIV-1.

RESULTS:

Balanced selection of challenge animals

Our goal was to assess the capability of vaccine-elicited Tier 2 nAbs to protect from homologous Tier 2 challenge with neutralization-resistant, pathogenic $SHIV_{BG505}$ (Li et al., 2016). We previously developed a protocol for the reliable induction of nAbs and immunized 78 NHPs (Pauthner et al., 2017), inducing varying levels of autologous Tier 2 nAb titers after three immunizations with native-like BG505 Env trimers (de Taeye et al., 2015; Kulp et al., 2017; Torrents de la Peña et al., 2017). To design a challenge study powered to detect differences between NHPs with either high or low BG505 nAb titers, we selected six NHPs that were among the top neutralizers and carefully matched them as closely as possible, in terms of gender, age and weight, with six low nAb titer animals that received similar or identical immunogens (Figure S1, A to C). We note that none of the protective or viral breakthrough or antibody kinetic effects described below could be associated with a particular immunogen; as will be seen, observed effects are primarily associated with nAb titer. We further enrolled 12 unimmunized control animals into the study. All animals were genotyped for Mamu and TRIM-5α alleles associated with host restriction in non-human primates (Table S1).

Design of the $SHIV_{BG505}$ challenge study

To identify a challenge dose that reliably infects unimmunized control animals, we performed a pilot study by intrarectally (IR) inoculating two groups of six macaques at weekly intervals with either 0.5×10^8 or 1.4×10^7 virions of the $SHIV_{BG505}$ S375Y challenge

144 virus grown in rhesus $CD4^+$ T cells (Figure S2). For the main study, we selected a
145 challenge dose of 1.4×10^7 virions (1ml of 1:75 diluted challenge stock), since it infected
146 at least 4/6 animals following the 1st challenge and the remaining two animals after the
147 2nd challenge in the pilot study. To maximize nAb titer levels in NHPs prior to challenge,
148 high and low nAb titer animals each received a fourth immunization with the previously
149 used immunogens, adjuvanted with an ISCOMATRIX-like saponin (Figure 1A). All NHPs
150 responded with increased autologous nAb titers two weeks post-boost. High and low nAb
151 titer animals continued to show significantly different geometric mean ID_{50} titers of 1:3790
152 and 1:103 to BG505 S375Y pseudovirus (p=0.002, Figure 1B), respectively.
153 Neutralization titers to rhesus $CD4^+$ T-cell grown $SHIV_{BG505}$ S375Y challenge stock were
154 ~30-fold lower, with significantly different geometric mean titers of 1:102 and < 1:10 when
155 tested on TZM-bl target cells (p=0.002, Figure 1C), respectively.

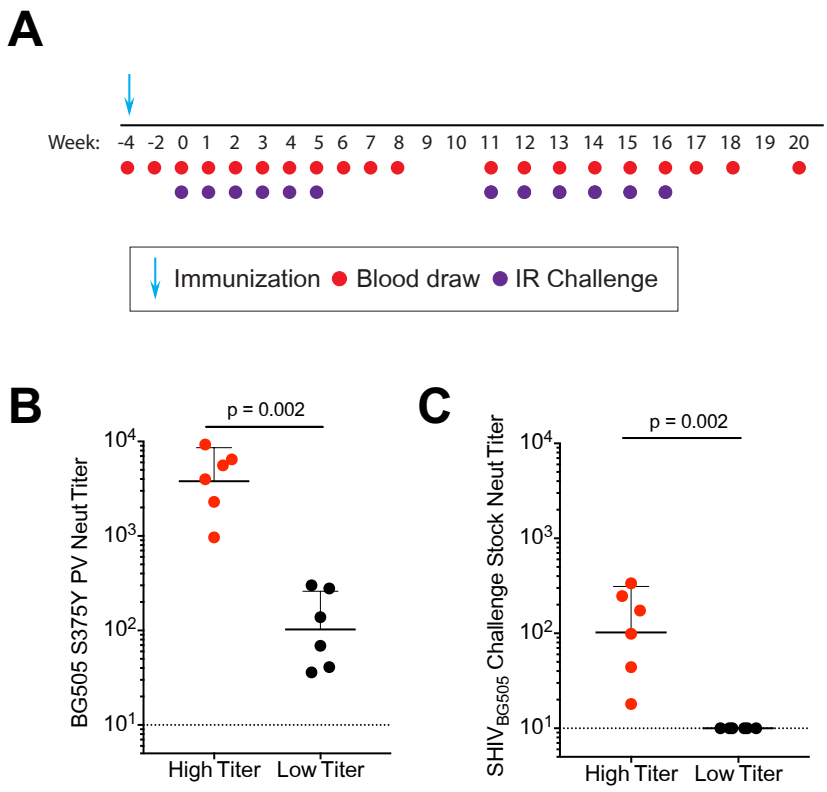

156

157 **Figure 1. Challenge study design.** (A) Animals, except for the controls, received a
158 booster immunization using the same immunogen that had last been used during the
159 preceding immunization study (Pauthner et al., 2017), typically 100µg SOSIP trimer
160 adjuvanted in IscoMIT. Intrarectal (IR) challenges with $SHIV_{BG505}$ S375Y commenced 4
161 weeks thereafter. All groups of animals received 6 IR challenges starting at week 0. High
162 nAb titer animals that had undetectable serum viral loads at week 6 received a second
163 set of 6 weekly IR challenges starting week 11. (B-C) Serum neutralizing ID_{50} titers in
164 high and low nAb titer animals at week -2: BG505 S375Y pseudovirus (B) and rh-CD4-
165 grown $SHIV_{BG505}$ S375Y challenge stock. (C). Shown are geometric means with
166 geometric SD, significant differences were determined using two-tailed Mann-Whitney U
167 tests.

Robust protection of high nAb titer group NHPs

Four weeks after the booster immunization, all animals received six weekly IR challenges with $SHIV_{BG505}$. To maximize comparability, viral loads for all animals and time points were simultaneously measured at weeks 6 and 20 (Figure 2, A to C). 5/6 concurrent unimmunized control animals were infected after the 1st challenge and the remaining animal became viremic after the 2nd challenge (Figure 2A). Combined with the unimmunized control NHPs of the dose-matched titration group (Figure S2), at least 9 of 12 unimmunized animals became infected following a single challenge, which approximates to an animal infectious dose of 75% (AID_{75}) (Table S2). Thus, the dose of 1.4×10^7 $SHIV_{BG505}$ virions per IR inoculation employed in this study sets a relatively high bar for protection. Unimmunized control animals showed high peak viremia (geometric mean of 5.5×10^6 copies/ml) and consistent set point viral loads in the range of 9.8×10^2 – 4.7×10^4 (geometric mean of 6.2×10^3) at 12 weeks post-infection (Figure 2, A and E, Figure S2).

2/6 low nAb titer animals became infected after the first challenge and the remaining four animals became viremic following the second challenge (Figure 2B), indicating that low nAb titer animals had a possible mild reduction in per-exposure risk compared to unimmunized controls, but the difference was not significant (Figure 2D, Table S3). However, low nAb titer animals had significantly lowered peak viral loads compared to unimmunized controls (1.5×10^5 vs. 5.5×10^6 copies/ml) ($p = 0.001$, Figure 2, E and F).

In contrast, high nAb titer animals showed highly significant protection from challenge following the first set of challenges at week 8 (Figure 2D, Table S3). Except for

191 macaque 12-143, no animals showed viremia at week 6 and were therefore scheduled to
192 receive a second set of six challenges starting at week 11. The goal of the second
193 challenge set was to assess the duration of protection and to estimate a protective nAb
194 titer threshold as nAb titers declined over time. Over the course of both challenge sets,
195 four initially high nAb titer animals became viremic, after 3, 6, 10 and 12 virus inoculations;
196 however, two animals showed complete sterilizing protection (Figure 2C). In addition,
197 infected high-titer macaques showed significantly lowered peak viremia compared to
198 unimmunized controls (3.2×10^4 vs 5.5×10^6 copies/ml; $p = 0.01$, Figure 2, E and F),
199 similar to the low nAb titer animals. We theorize that sub-protective levels of serum nAbs
200 at the time of infection, as well as activation of vaccine-induced memory B cells leading
201 to the rapid production of Abs, likely curtail emerging primary viremia, thus reducing peak
202 viral loads.

203 The protection from infection for high nAb titer animals was highly significant
204 compared to unimmunized controls after both 6 and 12 challenges ($p < 0.0001$, Figure
205 2D, Table S3) and animals in this group remained uninfected for a median of 11
206 challenges (Table S3). It should be emphasized that for all vaccinated animals, nAb titers
207 declined throughout the challenge schedule, unless animals became infected as detailed
208 below. In this respect, our study distinguishes itself from those in which antibody titers
209 leveled off prior to challenge, as a result of the short 4-week interval here between final
210 immunization and first challenge. However, we deliberately took advantage of declining
211 nAb titers to determine a nAb-mediated threshold of protection.

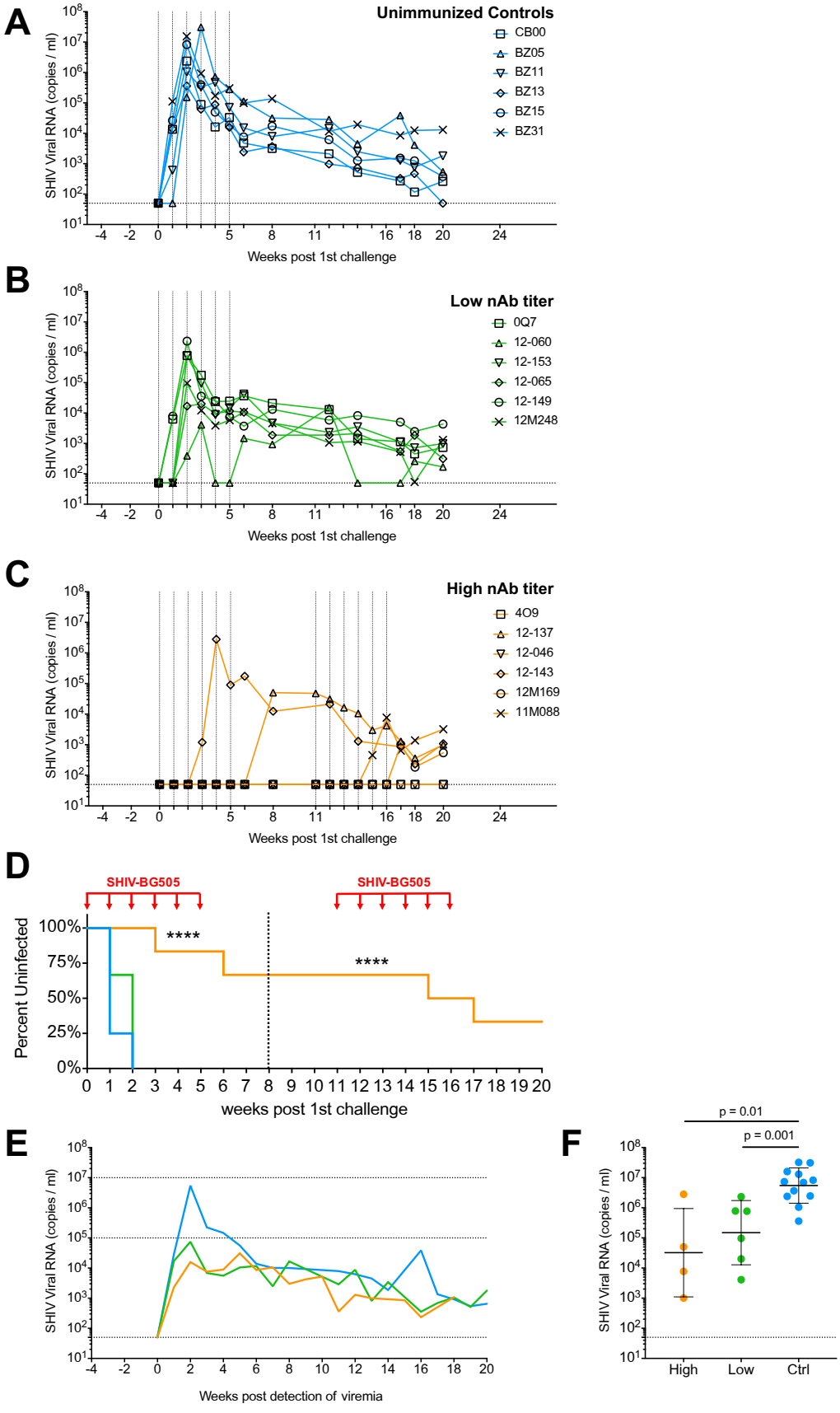

212

213 **Figure 2. High nAb titer animals show robust protection.** Viral loads of animals
214 throughout the challenge schedule: unimmunized concurrent controls (**A**), low nAb titer
215 (**B**) and high nAb titer macaques (**C**). IR challenges are indicated with vertical dotted
216 lines. Horizontal dotted lines denote the limit of detection. (**D**) Kaplan-Meier curves
217 indicating percent uninfected animals over the duration of the study. Challenge time
218 points are indicated with red arrows. The high nAb titer group infection-rate was
219 statistically different from the low nAb titer and unimmunized control groups. **** = $p <$
220 0.0001. Statistics were calculated for both the first (dotted line at week 8) and second
221 challenge sets (see Table S3) (**E**) Geometric mean viral loads of indicated groups,
222 normalized to the detection of viremia in the blood. Horizontal lines at 10^5 and 10^7 viral
223 RNA copies/ml serve as visual aids. (**F**) Comparison of peak viral loads between high
224 nAb titer (high), low nAb titer (low), and unimmunized (ctrl) animals. Geometric mean
225 titers are shown with geometric standard deviations. Significant differences were
226 determined using two-tailed Mann-Whitney U tests.

227

228 **Tier 2 nAb titers correlate with protection**

229 Unimmunized control animals developed BG505 S375Y pseudovirus ID_{50} nAb titers 8-12
230 weeks postinfection in response to $SHIV_{BG505}$ S375Y infection (Figure 3A). By
231 comparison, vaccine-induced nAb titers in low titer animals initially declined, but then
232 began to rise only 1-2 weeks postinfection, i.e. much more rapidly than in unimmunized
233 animals (Figure 3B). The early rise of nAb titers following infection of low nAb titer animals
234 is thus likely due to recall responses of BG505 Env immunogen-induced memory B cells.

Interestingly, BG505 nAb titers rose to substantially higher ID_{50} titers (3/6 animals >1:750) than previously achieved by four immunizations of these six animals with ISCOMs-adjuvanted BG505 native-like Env trimers (Figures 1B, 3B, S1B). The marked increases in BG505 nAb titers following infection suggest that outbred macaques that did not respond well to vaccination were not inherently incapable, by genetic or other means, of developing high nAb titer responses, although this conclusion should be caveated by the observation that antigen dose and delivery vary greatly between vaccination and natural infection. Better immunogen presentation and more targeted adjuvants are likely needed to increase the reliability of high nAb titer development, and to address current shortcomings in the durability of nAb responses induced by protein-only immunizations (Havenar-Daughton et al., 2017).

High nAb titer animals that became infected showed a comparable increase in BG505 S375Y nAb titers ~1-4 weeks following infection. The only exception was animal 12-137, who suppressed viremia for 3 weeks following challenge at week 5, and thus delayed a surge in nAb titers until week 11 (Figure 3C). Animal 12-143, which became viremic at week 3, showed only a small rise in nAb titers at week 6, suggesting possible rapid viral escape. PacBio sequencing of viral species in 12-143 plasma at week 8 in fact revealed that >95% of sequenced *env* genomes contained putative escape mutations at residues 168 and 192 (Figure S3A). Similarly, *env* genomes in 12-137 plasma at weeks 12 and 16 showed putative escape mutations at residues 354 and 356, flanking the N355 glycan, which coincided with onset of nAb titer decay at week 12 (Figure S3B, Figure 3C). NAb specificities to the N355-region were observed in BG505 SOSIP immunized rabbits (Klasse et al., 2018), and were detected in week 0 plasma of animal 12-137 using electron

258 microscopy based serum mapping (Figure S3C) (Bianchi et al., 2018). We could further
259 show that the observed viral point mutations do confer neutralization resistance to sera
260 from the respective animals (Figure S3D-E). Animals 12M169 and 12M088, which
261 become infected at weeks 16 and 14, respectively, exhibited slow declines in vaccine-
262 induced nAb titers which then rose following infection (Figure 3C). The nAb titers of fully
263 protected animals 12-046 and 4O9 (Figure 3D) initially declined and then plateaued at
264 ~1:800 around week 10 and remained stable for the remainder of the study. This trend
265 was mirrored in longitudinal ELISA EC_{50} binding titers. (Figure S3F-G). Uninfected
266 animals retained robust nAb titer levels over 1 year past the final immunization (Figure
267 S3H).

268 The differences in both BG505 S375Y pseudovirus as well as $SHIV_{BG505}$ challenge
269 stock neutralization ID_{50} titers between high and low nAb titer animals at week -2 were,
270 as anticipated, highly significant (Figure 1, B and C). Peak nAb titers at week -2 accurately
271 predicted the duration of protection, identifying nAb titers as the primary correlate of
272 protection ($p < 0.0001$, Figure 4A). Using the BG505 S375Y pseudovirus assay, a
273 statistically significant difference was found between nAb titers in immunized animals 7d
274 prior to onset of viremia and animals that remained uninfected until week 20 ($p = 0.03$,
275 Figure 4B, Figure S4A).

276 To numerically quantify the relationship between BG505 S375Y pseudovirus nAb
277 titers and likelihood of infection, we developed a modified Bayesian logistic regression
278 model using the neutralization and viral load data from all three animal groups (Figure
279 4C, S5). The posterior median infection probability at the limit of nAb titer detection was
280 77%, agreeing closely with an estimated animal infectious dose of 75% in unimmunized

281 controls. A median per-challenge infection probability of 50% was attained with ID_{50} titers
282 of 1:90, which agrees well with the often-quoted 50% protective ID_{50} titer of ~1:100,
283 derived from bnAb passive transfer studies (Hessell et al., 2018; Moldt et al., 2012; Parren
284 et al., 2001; Pegu et al., 2014; Shingai et al., 2014), although we note that various different
285 neutralization assays with differing sensitivities were employed in these studies. To
286 achieve an infection probability of 10%, or 90% protection, an ID_{50} titer of 1:476 (CI: 272-
287 991) was required. In agreement with our model, animals with nAb titers above ~1:500
288 remained protected over all 12 challenges, while animals with nAb titers below 1:200
289 generally became infected with only 1-2 challenges. For the rhesus $CD4^+$ T cell grown
290 $SHIV_{BG505}$ S375Y virus stock, an ID_{50} titer of ~1:30 (Figure S4B) was the protection
291 threshold. The observed disparity between pseudovirus and PBMC-grown virus assays
292 was relatively large compared with that reported for many mAbs but still within previously
293 observed ranges (Figure S4C) (Cohen et al., 2018; Provine et al., 2012). Thus, Tier 2
294 nAb titers both predicted and correlated with protection from infection.

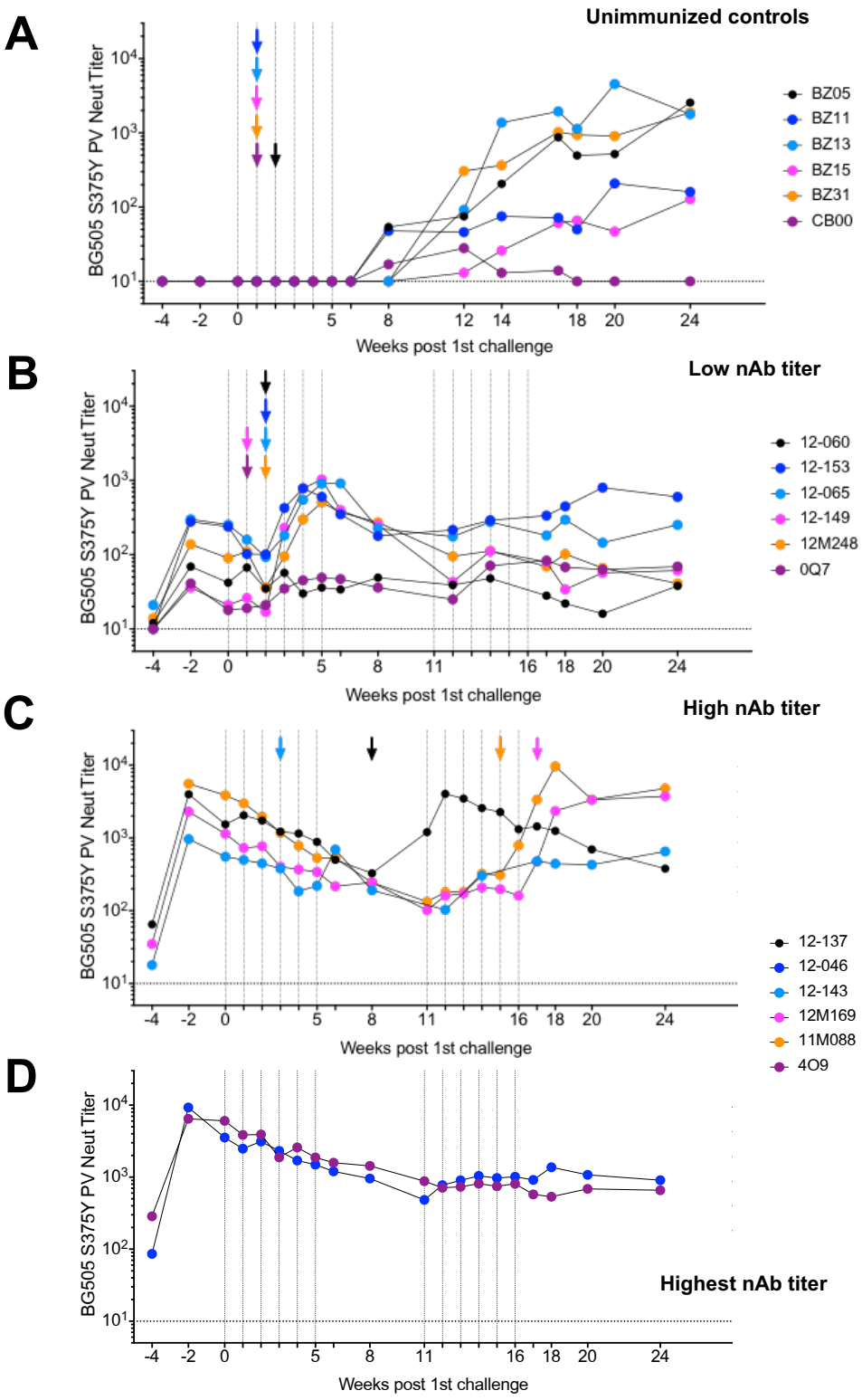

295

296 **Figure 3: Longitudinal development of autologous Tier 2 nAb titers.** (**A-D**) Serum

297 neutralizing antibody titers throughout the challenge schedule: BG505 S375Y

298 pseudovirus ID_{50} nAb titers rise 8-12 weeks post infection in unimmunized animals (**A)** or
299 1-2 weeks following detection of viremia in low nAb titer animals (**B**). BG505 S375Y
300 pseudovirus ID_{50} nAb titers in macaques that became infected over time (**C**) or showed
301 sterilizing protection (**D**). In (**D**), nAb titers peaked at week -2 following a final boost at
302 week -4 and slowly declined until ~week 10 after which titers plateaued and remained
303 stable for the duration of the study. Macaques infected during the second set of
304 challenges displayed similar nAb titer plateaus as protected animals until infection.
305 Animals that became infected showed a surge in nAb titer followed by a slow decline e.g.
306 animal 12-137. First detection of plasma viremia is indicated by colored arrows
307 corresponding to the animal IDs shown in the respective figure legends.

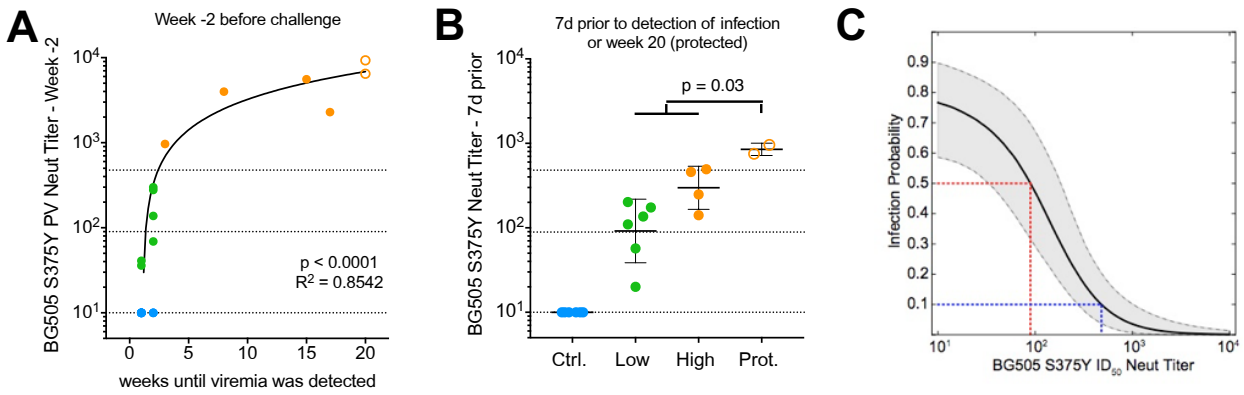

Figure 4. Protection is associated with serum nAb titers greater than ~1:500. (**A**) BG505 S375Y pseudovirus ID_{50} nAb titers at week -2 predict and correlate with the duration of protection. (**B**) BG505 S375Y pseudovirus ID_{50} nAb titers of control (Ctrl.), low nAb titer (Low) and high nAb titer (High) animals 7 days before detection of viral load in the blood and at week 20 for protected (Prot.) animals that showed sterilizing protection throughout the study. All nAb titers were measured in TZM-bl assays. Correlations were calculated using Spearman correlation tests, comparisons between groups were calculated using Mann-Whitney U tests. Horizontal lines indicate 50% and 90% protective nAb titers as defined in 3G. (**C**) The 5%, median, and 95% credible intervals (CI) are shown for the probability of infection in relation to serum BG505 S375Y pseudovirus nAb titer, inferred using a modified Bayesian logistic regression model (see figs. S10-S12). The posterior median infection probability at the limit of nAb titer detection was 77%, agreeing closely with an estimated animal infectious dose of 75% in unimmunized animals. A median infection probability of 50% is attained with an ID_{50} titer of 1:90 (red line, CI: 34-178), and an infection probability of 10% with an ID_{50} titer of 1:476 (blue line, CI: 272-991).

T cell activity and serum antibody-dependent cell-mediated cytotoxicity (ADCC) do not correlate with protection

We further investigated other parameters that may have contributed to protection. Robust Env-specific $CD4^+$ T cell responses were elicited by BG505 Env trimer immunization and were equivalent in magnitude between the high and low nAb titer groups of immunized animals before challenge (Figure 5, A and E, Figure S6, A to C). Cytokine-producing Env-specific $CD4^+$ T cells were also comparable between the two groups of immunized animals before challenge ($IFN\gamma^+$, Figure 5, B and F; TNF^+CD40L^+, Figure 5, C and G, Figure S6D) and protein vaccine-elicited Env-specific $CD8^+$ T cells were undetectable, as expected (Figure 5,D and H). Thus, Env-specific $CD4^+$ T cells or $CD8^+$ T cells are not a correlate of protection.

Concerns have been raised about vaccine-elicited $CD4^+$ T cell responses enhancing susceptibility to infection by HIV (Fauci et al., 2014; Hu et al., 2014) or SIV (Fouts et al., 2015; Staprans et al., 2004) by providing more targets for infection at the mucosal site of transmission (Bukh et al., 2014; Carnathan et al., 2015; Martins and Watkins, 2017; Qureshi et al., 2012), most likely due to the presence of activated Th1 cells in the mucosa, which was correlated with CCR5, α4β7, or proliferation in different studies. Minimal Th1 cells were detected in the BG505 Env trimer immunized animals ($IFN\gamma^+$ $CD4^+$ T cells, Figure 5, B & F). $CCR5^+$, $Ki67^+$ or $Ki67^+/\alpha4\beta7^+$ $CD4^+$ T cells in peripheral blood prior to challenge were not correlated with susceptibility to infection or protection (Figure S6, E to H). Thus, we observed robust protection of high nAb titer animals against a mucosal SHIV challenge despite substantial levels of Env-specific vaccine-induced $CD4^+$ T cells in peripheral blood at 4 weeks after the final immunization.

349 The difference in our study may be due to a lack of Th1 or mucosal homing CD4+ T cells
350 in response to the protein vaccine, compared to previously used viral vectors (Bukh et al.,
351 2014; Carnathan et al., 2015; Fauci et al., 2014; Hu et al., 2014; Staprans et al., 2004).
352 Alternatively, nAb-mediated protection against HIV/SIV may more readily overcome
353 possible adverse consequences of increased numbers of activated $CD4^+$ T cell targets
354 than the non-neutralizing Abs (nnAbs) raised in the earlier studies.

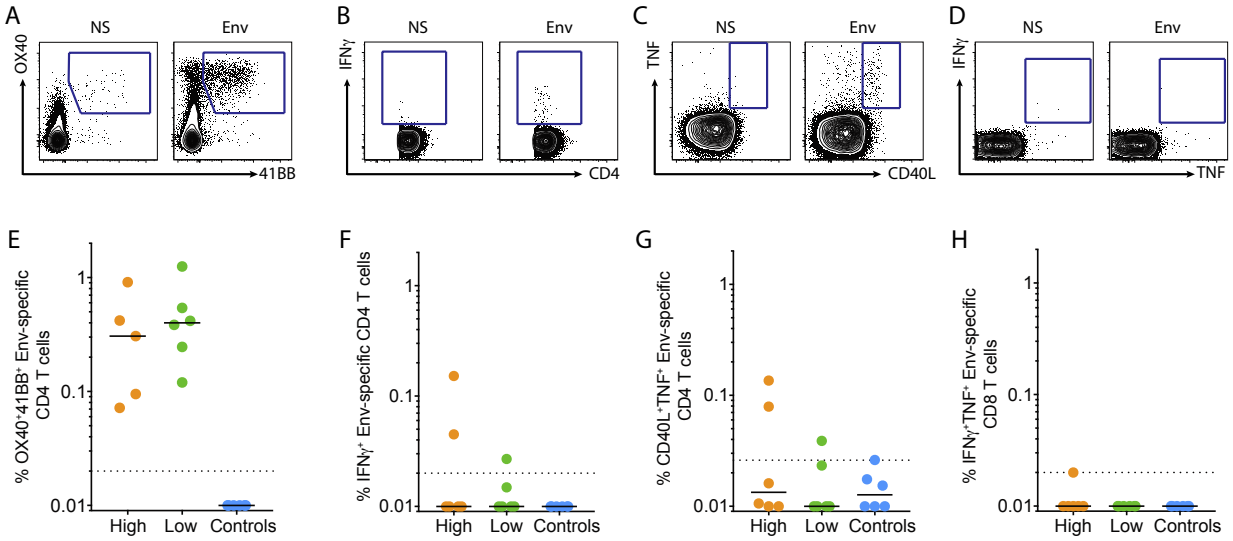

Figure 5. HIV Env-specific CD4$^+$ T cells and Env-specific CD8$^+$ T cells at week 0 are not associated with the observed protection from infection. (**A-C**) Representative flow plots of Env-specific CD4 T cells from week 0 PBMCs: using an OX40/4-1BB AIM assay (Reiss et al., 2017) (**A**), ICS assay for IFNγ (**B**), and ICS assay for TNF/CD40L (**C**) when not stimulated (ns) versus stimulated with antigen (Env). (**D**) Representative flow plot of IFNγ and TNF expression in CD8 T cells by ICS when not stimulated (ns) versus stimulated with antigen (Env). (**E-G**) Quantification of the percent of CD4 T cells that are Env-specific based on: OX40/4-1BB (**E**), IFNγ (**F**), or CD40L/TNF (**G**) expression. (**H**) Quantification of the percent of CD8 T cells that are Env-specific based on IFNγ and TNF expression. Signal from the unstimulated condition was subtracted from the antigen-specific signal for each sample. Each dot represents an individual animal.

To investigate possible contributions of ADCC of both nAbs and nnAbs, we tested animal sera in two infection-based assays; $SHIV_{BG505}$-infected CEM.NKR luciferase reporter cells (Alpert et al., 2012) (Figure 6A) and flow cytometric analysis of ADCC in $p27^+$ $SHIV_{BG505}$-infected CEM.NKR target cells (Veillette et al., 2014) (Figure 6B). Using either assay, we failed to detect meaningful ADCC activity at week 0 with the exception of a single animal, 12-149, which was a low titer animal whose ADCC activity was non-specific and included activity against control $SIV_{mac}239$ (Figure S7A). The absence of observed ADCC activity can be partially explained by the Tier 2 character of BG505 Env. In native Env trimer-based ADCC assays, nnAb and Tier 1 nAbs fail to mediate ADCC-activity against, hard-to-neutralize Tier 2 HIV isolates, as previously reported (Bredow et al., 2016; Ding et al., 2016). In addition, ADCC activation in infection-based assays varies strongly depending on the targeted epitope, which is likely related to the Ab binding stoichiometry to the epitope and the ability to cross-link sparse trimers on the virion surface (Figure S7B-D) (Bredow et al., 2016; Ding et al., 2016).

Unlike infection-based assays, ADCC killing measured on CEM.NKR target cells coated with BG505 gp120 was robust, but did not distinguish between high and low nAb titer animals and, therefore, was not associated with protection (Figure 6C). ADCC killing of gp120-coated cells did correlate with BG505 gp120 binding, indicating that gp120-binding antibodies are sufficient to induce ADCC in this assay (Figure 6D), but cannot mediate ADCC to native membrane-bound Env on infected cells. Thus, ADCC unlikely contributes to protection. We also observed considerable staining of $p27^-$ uninfected bystander T cells by both mAbs and animal sera, which appears to result from antibody binding to shed gp120 from infected cells that is captured on CD4 of uninfected cells

(Figure S7D) (Richard et al., 2018). Overall, these results suggest caution in the use of ADCC assays that are either based on recombinant gp120 or gp140 binding, rather than native Env on virus-infected cells, or cannot distinguish productively infected from uninfected bystander cells (Ackerman et al., 2016; Ferrari et al., 2011; Huang et al., 2016; Johansson et al., 2011; Kristensen et al., 2018). We note that the results pertain to ADCC; there remains the possibility that other Fc-mediated effector functions might contribute to protection.

Lastly, we determined BG505 SOSIP.664 (Figure 6E), V3-peptide (Figure 6F), and BG505 gp120 binding titers (Figure 6G) for all groups at week 0 since V3-targeting antibodies (Balasubramanian et al., 2018), and binding antibodies in general have been associated with anti-viral activities (Excler et al., 2014). No significant differences between high and low neutralizer animals were detected.

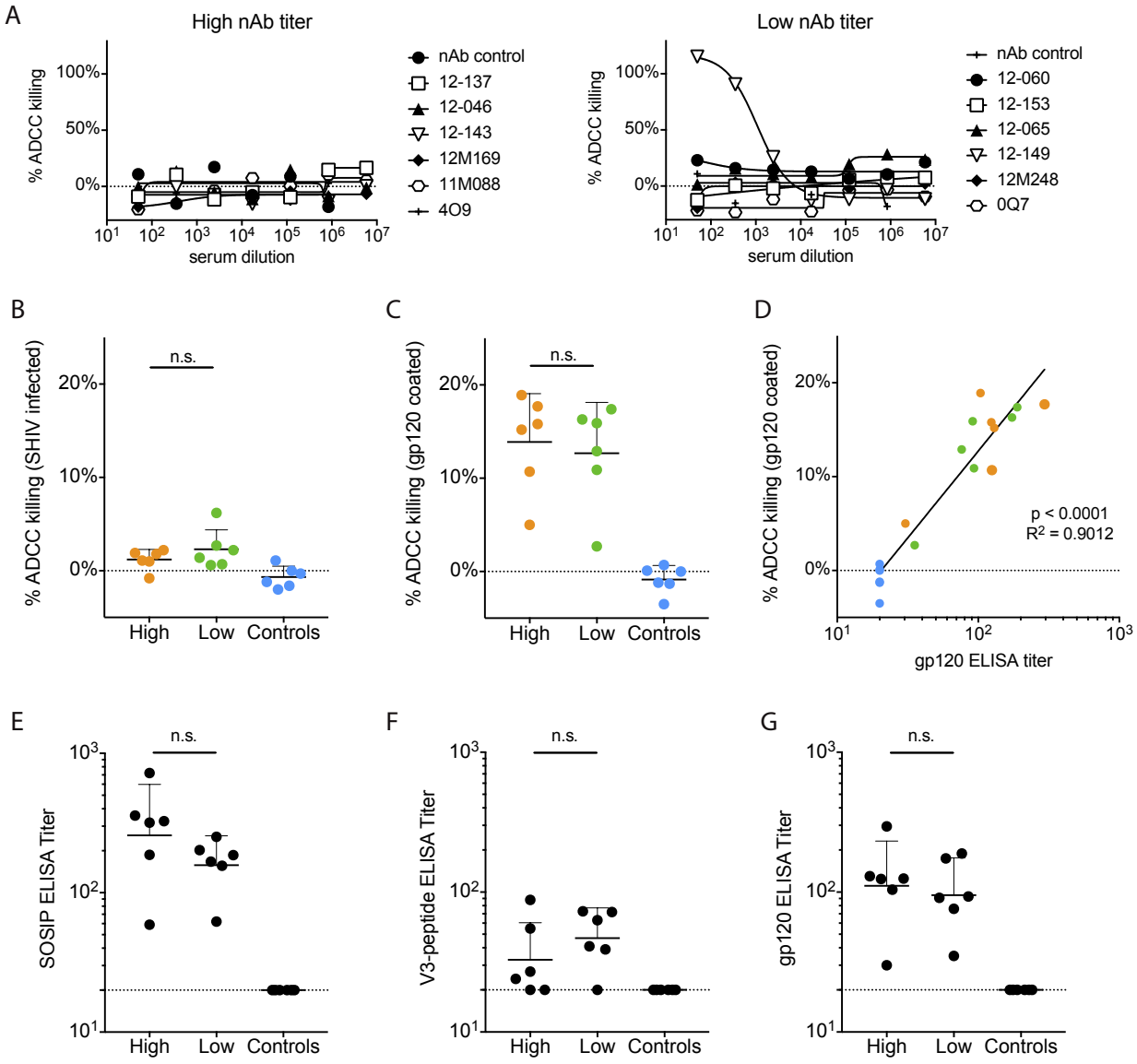

Figure 6: ADCC activity at week 0 measured in SHIV-infection as well as gp120-based assays is not associated with the observed protection from infection. (**A-G**) ADCC-activity from sera of high and low nAb titer as well as control animals at week 0. ADCC activity in titrated sera was measured using $SHIV_{BG505}$ challenge stock infected CEM.NKR luciferase-reporter target cells and CD16 transfected KHYG-1 effector cells (**A**) or in 1:250 diluted sera by flow cytometric analysis of ADCC activity in either $p27^{+}$ $SHIV_{BG505}$-infected CEM.NKR cells (**B**) or BG505 g120-coated CEM.NKR cells (**C**), using

PBMCs as effector cells. ADCC-activity in BG505 gp120-coated CEM.NKR cells correlated with BG505 gp120 binding titers (**D**). (**E-G**) ELISA EC_{50} binding titers to: BG505 SOSIP.664 (**E**), BG505 V3-peptide (**F**) or BG505 gp120 (**G**). Sera from high and low titer animals, as well as unimmunized control animals were tested for ELISA binding titers at week 0. Correlations were calculated using Spearman correlation tests, comparisons between groups were calculated using Mann-Whitney U tests.

DISCUSSION

Vaccine protection against HIV in humans and against SIV and SHIV in macaques has been associated with non-neutralizing antibodies (Barouch et al., 2015; Haynes et al., 2012). Here, we demonstrate that vaccine-induced Tier 2 nAbs, but not other antibody parameters such as V3 binding titers, antibody-dependent cellular cytotoxicity (ADCC), or induction of T cell activity, are a correlate of protection from homologous $SHIV_{BG505}$ infection in macaques. Notably, we employed a challenge dose of virus corresponding to an AID_{75}, which sets a relatively high bar for protection, given that most animals (~53%) in the control arm were estimated to have been productively infected by two or more viruses (Table S2). Similar rates of multivariant virus transmission have been reported in men who have sex with men and injection drug users who acquire HIV-1 infection (38% and 60% with a MOI of 2 or higher, respectively), while heterosexual cohorts show lower multivariant transmission frequencies (~19%). Thus, our model mimics the conditions of productive transmission events, underlining the physiological relevance of the challenge dose that we used (Bar et al., 2010; Li et al., 2010).

We show, in the model system described, that animals remain protected from SHIV infection in a nAb titer-dependent manner, which suggests a strong relationship between circulating nAb titers in the blood and protection from mucosal challenge with difficult-to-neutralize, Tier 2 $SHIV_{BG505}$. At the same time, our data suggest that vaccine protection can occur in the absence of ADCC. We show that unprotected animals have relatively high levels of ADCC when measured in a widely used ADCC assay that uses target cells coated with monomeric gp120, but not with $SHIV_{BG505}$ infected target cells. We further provide evidence that adjuvanted protein immunization with HIV Env can induce nAb titers

that are durable and protective over longer periods of time, if high initial nAb titers following immunization can be reached. This has been a major concern in the HIV vaccine field (Sundling et al., 2013), but also for other protein-based vaccines, such as recombinant influenza vaccines (Krammer and Palese, 2015). Importantly, we identified that a serum ID_{50} nAb titer of ~1:500 against the homologous BG505 S375Y pseudovirus at the time of challenge can confer reliable protection of > 90%, meaning that 9 of 10 challenges with a physiologically-relevant AID_{75} dose would not result in infection. Finally, protection is observed for polyclonal neutralizing Ab responses that, as above and earlier {Pauthner:2017fd}, target multiple specificities on Env and not simply the previously described glycan hole on BG505 Env.

In conclusion, we provide evidence that protein immunization with native-like Env trimers can induce potent and protective nAb titers in the SHIV/macaque model. Thus, nAb-mediated protection from Tier 2 virus challenge is not limited to bnAbs, which are generally focused to a single site of vulnerability and have a defined effector-function profile, but can also be accomplished by polyclonal autologous nAb responses of sufficient magnitude and specificity, which comprise a broad range of neutralizing and non-neutralizing antibody lineages to various, often overlapping epitopes that interact in both synergistic or competitive ways (Klasse et al., 2018; Pauthner et al., 2017; Sanders et al., 2015; Torrents de la Peña et al., 2018). The protective nAb titer threshold against the homologous challenge virus that we determined is in rough accord with passive antibody transfer studies and provides a benchmark for comparison with upcoming antibody protection studies against HIV in humans (www.ampstudy.org).

ACKNOWLEDGEMENTS:

We would like to thank Laura Pruyn and Joan Allmaras for excellent administrative support. The funding for this study was provided by NIAID UM1AI100663 (Center for HIV/AIDS Vaccine Immunology and Immunogen Discovery). The Bill & Melinda Gates (OPP1084519) and the International AIDS Vaccine Initiative helped support the design of some immunogens used in this study. This work was further supported by the National Institutes of Health grants AI121135 (DTE), AI124377, AI126603, AI128751 (DHB), OD011106 (Wisconsin National Primate Research Center) and grant OPP1145046 from the Bill & Melinda Gates Foundation (GMS). AF work was supported by CIHR foundation grant #352417. AF is the recipient of a Canada Research Chair on Retroviral Entry RCHS0235. JP is the recipient of a CIHR Fellowship Award. BM was supported by grants R00AI120851 and UM1AI068618 from the National Institute of Allergy and Infectious Diseases. PacBio SMRT sequencing was performed with the support of the Translational Virology Core at the UC San Diego Center for AIDS Research (P30 AI036214), and the IGM Genomics Center, University of California, San Diego, La Jolla, California.

AUTHOR CONTRIBUTIONS:

The TSRI CHAVI-ID immunogen working group consisting of SC, WRS, ABW, IAW, RTW and DRB, with the assistance of MGP, STB, GMS and DHB designed the challenge study and laid out the experimental strategy. JPN and DHB oversaw all rhesus macaque immunizations and challenges, including sample acquisition, processing, storage and distribution. PA and DHB performed and oversaw viral load assays. HL and GMS designed and produced the SHIVBG505 challenge stock. CAC, DWK and TT with oversight from DJI, ABW, WRS and RWS designed and produced the boosting

485 immunogens for the study. MGP, RB, JHL and DRB designed HIV pseudovirus mutants
486 and performed and oversaw neutralization experiments as well as ELISA binding
487 experiments. CHD, SMR and SC performed and oversaw flow cytometric analysis of T
488 cell activation. JP, RN and BVB with oversight from DTE, LH and AF performed ADCC
489 assays. BN and MB with oversight from LH and ABW performed serum negative-stain
490 EM analysis. BM and MGP performed statistical analysis of data sets. MGP, JPN, CHD,
491 BM, SMR, JP, RN, BVB, TT, STB, DTE, LH, AF, IAW, RTW, DJI, WRS, ABW, RWS, SC,
492 GMS, DHB and DRB analyzed data sets and contributed edits to the manuscript. MGP,
493 SC and DRB wrote the manuscript.

494

495 **DECLARATION OF INTERESTS**

496 The authors declare no competing interests

497

498 **REFERENCES:**

499 Abrahams, M.R., Anderson, J.A., Giorgi, E.E., Seoighe, C., Mlisana, K., Ping, L.H.,
500 Athreya, G.S., Treurnicht, F.K., Keele, B.F., Wood, N., Salazar-Gonzalez, J.F.,
501 Bhattacharya, T., Chu, H., Hoffman, I., Galvin, S., Mapanje, C., Kazembe, P.,
502 Thebus, R., Fiscus, S., Hide, W., Cohen, M.S., Karim, S.A., Haynes, B.F., Shaw,
503 G.M., Hahn, B.H., Korber, B.T., Swanstrom, R., Williamson, C., CAPRISA Acute
504 Infection Study Team, Center for HIV-AIDS Vaccine Immunology Consortium, 2009.
505 Quantitating the multiplicity of infection with human immunodeficiency virus type 1
506 subtype C reveals a non-poisson distribution of transmitted variants. J. Virol. 83,
507 3556–3567. doi:10.1128/JVI.02132-08
508 Ackerman, M.E., Mikhailova, A., Brown, E.P., Dowell, K.G., Walker, B.D., Bailey-
509 Kellogg, C., Suscovich, T.J., Alter, G., 2016. Polyfunctional HIV-Specific Antibody
510 Responses Are Associated with Spontaneous HIV Control. PLoS Pathog. 12,
511 e1005315. doi:10.1371/journal.ppat.1005315
512 Alpert, M.D., Heyer, L.N., Williams, D.E.J., Harvey, J.D., Greenough, T., Allhorn, M.,
513 Evans, D.T., 2012. A novel assay for antibody-dependent cell-mediated cytotoxicity

514 against HIV-1- or SIV-infected cells reveals incomplete overlap with antibodies
515 measured by neutralization and binding assays. J. Virol. 86, 12039–12052.
516 doi:10.1128/JVI.01650-12
517 Balasubramanian, P., Williams, C., Shapiro, M.B., Sinangil, F., Higgins, K., Nàdas, A.,
518 Totrov, M., Kong, X.-P., Fiore-Gartland, A.J., Haigwood, N.L., Zolla-Pazner, S.,
519 Hioe, C.E., 2018. Functional Antibody Response Against V1V2 and V3 of HIV
520 gp120 in the VAX003 and VAX004 Vaccine Trials. Sci. Rep. 8, 542.
521 doi:10.1038/s41598-017-18863-0
522 Bar, K.J., Li, H., Chamberland, A., Tremblay, C., Routy, J.P., Grayson, T., Sun, C.,
523 Wang, S., Learn, G.H., Morgan, C.J., Schumacher, J.E., Haynes, B.F., Keele, B.F.,
524 Hahn, B.H., Shaw, G.M., 2010. Wide variation in the multiplicity of HIV-1 infection
525 among injection drug users. J. Virol. 84, 6241–6247. doi:10.1128/JVI.00077-10
526 Barnett, S.W., Barnett, S.W., Srivastava, I.K., Srivastava, I.K., Kan, E., Kan, E., Zhou,
527 F., Zhou, F., Goodsell, A., Goodsell, A., Cristillo, A.D., Cristillo, A.D., Ferrai, M.G.,
528 Ferrai, M.G., Weiss, D.E., Weiss, D.E., Letvin, N.L., Letvin, N.L., Montefiori, D.,
529 Montefiori, D., Pal, R., Pal, R., Vajdy, M., Vajdy, M., 2008. Protection of macaques
530 against vaginal SHIV challenge by systemic or mucosal and systemic vaccinations
531 with HIV-envelope. AIDS 22, 339–348. doi:10.1097/QAD.0b013e3282f3ca57
532 Barnett, S.W., Burke, B., Sun, Y., Kan, E., Legg, H., Lian, Y., Bost, K., Zhou, F.,
533 Goodsell, A., Megede, Zur, J., Polo, J., Donnelly, J., Ulmer, J., Otten, G.R., Miller,
534 C.J., Vajdy, M., Srivastava, I.K., 2010. Antibody-mediated protection against
535 mucosal simian-human immunodeficiency virus challenge of macaques immunized
536 with alphavirus replicon particles and boosted with trimeric envelope glycoprotein in
537 MF59 adjuvant. J. Virol. 84, 5975–5985. doi:10.1128/JVI.02533-09
538 Barouch, D.H., Alter, G., Broge, T., Linde, C., Ackerman, M.E., Brown, E.P., Borducchi,
539 E.N., Smith, K.M., Nkolola, J.P., Liu, J., Shields, J., Parenteau, L., Whitney, J.B.,
540 Abbink, P., Ng'ang'a, D.M., Seaman, M.S., Lavine, C.L., Perry, J.R., Li, W.,
541 Colantonio, A.D., Lewis, M.G., Chen, B., Wenschuh, H., Reimer, U., Piatak, M.,
542 Lifson, J.D., Handley, S.A., Virgin, H.W., Koutsoukos, M., Lorin, C., Voss, G.,
543 Weijtens, M., Pau, M.G., Schuitemaker, H., 2015. Protective efficacy of
544 adenovirus/protein vaccines against SIV challenges in rhesus monkeys. Science
545 349, 320–324. doi:10.1126/science.aab3886
546 Bianchi, M., Turner, H.L., Nogal, B., Cottrell, C.A., Oyen, D., Pauthner, M., Bastidas, R.,
547 Nedellec, R., McCoy, L.E., Wilson, I.A., Burton, D.R., Ward, A.B., Hangartner, L.,
548 2018. Electron-Microscopy-Based Epitope Mapping Defines Specificities of
549 Polyclonal Antibodies Elicited during HIV-1 BG505 Envelope Trimer Immunization.
550 Immunity 49, 288–300.e8. doi:10.1016/j.immuni.2018.07.009
551 Bredow, von, B., Arias, J.F., Heyer, L.N., Moldt, B., Le, K., Robinson, J.E., Zolla-Pazner,
552 S., Burton, D.R., Evans, D.T., 2016. Comparison of Antibody-Dependent Cell-
553 Mediated Cytotoxicity and Virus Neutralization by HIV-1 Env-Specific Monoclonal
554 Antibodies. J. Virol. 90, 6127–6139. doi:10.1128/JVI.00347-16
555 Bukh, I., Calcedo, R., Roy, S., Carnathan, D.G., Grant, R., Qin, Q., Boyd, S., Ratcliffe,
556 S.J., Veeder, C.L., Bellamy, S.L., Betts, M.R., Wilson, J.M., 2014. Increased
557 mucosal CD4+ T cell activation in rhesus macaques following vaccination with an
558 adenoviral vector. J. Virol. 88, 8468–8478. doi:10.1128/JVI.03850-13

559 Carnathan, D.G., Wetzel, K.S., Yu, J., Lee, S.T., Johnson, B.A., Paiardini, M., Yan, J.,
560 Morrow, M.P., Sardesai, N.Y., Weiner, D.B., Ertl, H.C.J., Silvestri, G., 2015.
561 Activated CD4+CCR5+ T cells in the rectum predict increased SIV acquisition in
562 SIVGag/Tat-vaccinated rhesus macaques. Proc. Natl. Acad. Sci. U.S.A. 112, 518–
563 523. doi:10.1073/pnas.1407466112
564 Cohen, Y.Z., Lorenzi, J.C.C., Seaman, M.S., Nogueira, L., Schoofs, T., Krassnig, L.,
565 Butler, A., Millard, K., Fitzsimons, T., Daniell, X., Dizon, J.P., Shimeliovich, I.,
566 Montefiori, D.C., Caskey, M., Nussenzweig, M.C., 2018. Neutralizing Activity of
567 Broadly Neutralizing Anti-HIV-1 Antibodies against Clade B Clinical Isolates
568 Produced in Peripheral Blood Mononuclear Cells. J. Virol. 92.
569 doi:10.1128/JVI.01883-17
570 de Taeye, S.W., Ozorowski, G., Torrents de la Peña, A., Guttman, M., Julien, J.-P., van
571 den Kerkhof, T.L.G.M., Burger, J.A., Pritchard, L.K., Pugach, P., Yasmeen, A.,
572 Crampton, J., Hu, J., Bontjer, I., Torres, J.L., Arendt, H., Destefano, J., Koff, W.C.,
573 Schuitemaker, H., Eggink, D., Berkhout, B., Dean, H., Labranche, C., Crotty, S.,
574 Crispin, M., Montefiori, D.C., Klasse, P.J., Lee, K.K., Moore, J.P., Wilson, I.A., Ward,
575 A.B., Sanders, R.W., 2015. Immunogenicity of Stabilized HIV-1 Envelope Trimers
576 with Reduced Exposure of Non-neutralizing Epitopes. 163, 1702–1715.
577 doi:10.1016/j.cell.2015.11.056
578 Del Prete, G.Q., Keele, B.F., Fode, J., Thummar, K., Swanstrom, A.E., Rodriguez, A.,
579 Raymond, A., Estes, J.D., LaBranche, C.C., Montefiori, D.C., KewalRamani, V.N.,
580 Lifson, J.D., Bieniasz, P.D., Hatziioannou, T., 2017. A single gp120 residue can
581 affect HIV-1 tropism in macaques. PLoS Pathog. 13, e1006572.
582 doi:10.1371/journal.ppat.1006572
583 Ding, S., Veillette, M., Coutu, M., Prévost, J., Scharf, L., Bjorkman, P.J., Ferrari, G.,
584 Robinson, J.E., Stürzel, C., Hahn, B.H., Sauter, D., Kirchhoff, F., Lewis, G.K.,
585 Pazgier, M., Finzi, A., 2016. A Highly Conserved Residue of the HIV-1 gp120 Inner
586 Domain Is Important for Antibody-Dependent Cellular Cytotoxicity Responses
587 Mediated by Anti-cluster A Antibodies. J. Virol. 90, 2127–2134.
588 doi:10.1128/JVI.02779-15
589 Eren, K., Weaver, S., Ketteringham, R., Valentyn, M., Laird Smith, M., Kumar, V.,
590 Mohan, S., Kosakovsky-Pond, S.L., Murrell, B., 2017. Full-Length Envelope
591 Analyzer (FLEA): A tool for longitudinal analysis of viral amplicons. bioRxiv.org.
592 doi:10.1101/230474
593 Excler, J.-L., Ake, J., Robb, M.L., Kim, J.H., Plotkin, S.A., 2014. Nonneutralizing
594 functional antibodies: a new “old” paradigm for HIV vaccines. Clin Vaccine Immunol
595 21, 1023–1036. doi:10.1128/CVI.00230-14
596 Fauci, A.S., Marovich, M.A., Dieffenbach, C.W., Hunter, E., Buchbinder, S.P., 2014.
597 Immunology. Immune activation with HIV vaccines. Science 344, 49–51.
598 doi:10.1126/science.1250672
599 Fenizia, C., Keele, B.F., Nichols, D., Cornara, S., Binello, N., Vaccari, M., Pegu, P.,
600 Robert-Guroff, M., Ma, Z.-M., Miller, C.J., Venzon, D., Hirsch, V., Franchini, G.,
601 2011. TRIM5α does not affect simian immunodeficiency virus SIV(mac251)
602 replication in vaccinated or unvaccinated Indian rhesus macaques following
603 intrarectal challenge exposure. J. Virol. 85, 12399–12409. doi:10.1128/JVI.05707-11

Ferrari, G., Pollara, J., Kozink, D., Harms, T., Drinker, M., Freel, S., Moody, M.A., Alam, S.M., Tomaras, G.D., Ochsenbauer, C., Kappes, J.C., Shaw, G.M., Hoxie, J.A., Robinson, J.E., Haynes, B.F., 2011. An HIV-1 gp120 envelope human monoclonal antibody that recognizes a C1 conformational epitope mediates potent antibody-dependent cellular cytotoxicity (ADCC) activity and defines a common ADCC epitope in human HIV-1 serum. J. Virol. 85, 7029–7036. doi:10.1128/JVI.00171-11

Fouts, T.R., Bagley, K., Prado, I.J., Bobb, K.L., Schwartz, J.A., Xu, R., Zagursky, R.J., Egan, M.A., Eldridge, J.H., LaBranche, C.C., Montefiori, D.C., Le Buanec, H., Zagury, D., Pal, R., Pavlakis, G.N., Felber, B.K., Franchini, G., Gordon, S., Vaccari, M., Lewis, G.K., DeVico, A.L., Gallo, R.C., 2015. Balance of cellular and humoral immunity determines the level of protection by HIV vaccines in rhesus macaque models of HIV infection. Proc. Natl. Acad. Sci. U.S.A. 112, E992–9. doi:10.1073/pnas.1423669112

Gautam, R., Nishimura, Y., Pegu, A., Nason, M.C., Klein, F., Gazumyan, A., Golijanin, J., Buckler-White, A., Sadjadpour, R., Wang, K., Mankoff, Z., Schmidt, S.D., Lifson, J.D., Mascola, J.R., Nussenzweig, M.C., Martin, M.A., 2016. A single injection of anti-HIV-1 antibodies protects against repeated SHIV challenges. Nature 533, 105–109. doi:10.1038/nature17677

Gruell, H., Bournazos, S., Ravetch, J.V., Ploss, A., Nussenzweig, M.C., Pietzsch, J., 2013. Antibody and antiretroviral preexposure prophylaxis prevent cervicovaginal HIV-1 infection in a transgenic mouse model. J. Virol. 87, 8535–8544. doi:10.1128/JVI.00868-13

Hansen, S.G., Piatak, M., Jr., Ventura, A.B., Hughes, C.M., Gilbride, R.M., Ford, J.C., Oswald, K., Shoemaker, R., Li, Y., Lewis, M.S., Gilliam, A.N., Xu, G., Whizin, N., Burwitz, B.J., Planer, S.L., Turner, J.M., Legasse, A.W., Axthelm, M.K., Nelson, J.A., Früh, K., Sacha, J.B., Estes, J.D., Keele, B.F., Edlefsen, P.T., Lifson, J.D., Picker, L.J., 2013. Immune clearance of highly pathogenic SIV infection. Nature 502, 1–7. doi:10.1038/nature12519

Havenar-Daughton, C., Carnathan, D.G., Torrents de la Peña, A., Pauthner, M., Briney, B., Reiss, S.M., Wood, J.S., Kaushik, K., van Gils, M.J., Rosales, S.L., van der Woude, P., Locci, M., Le, K.M., de Taeye, S.W., Sok, D., Mohammed, A.U.R., Huang, J., Gumber, S., Garcia, A., Kasturi, S.P., Pulendran, B., Moore, J.P., Ahmed, R., Seumois, G., Burton, D.R., Sanders, R.W., Silvestri, G., Crotty, S., 2016. Direct Probing of Germinal Center Responses Reveals Immunological Features and Bottlenecks for Neutralizing Antibody Responses to HIV Env Trimer. Cell Rep 17, 2195–2209. doi:10.1016/j.celrep.2016.10.085

Havenar-Daughton, C., Lee, J.H., Crotty, S., 2017. Tfh cells and HIV bnAbs, an immunodominance model of the HIV neutralizing antibody generation problem. Immunol. Rev. 275, 49–61. doi:10.1111/imr.12512

Haynes, B.F., Burton, D.R., 2017. Developing an HIV vaccine. Science 355, 1129–1130. doi:10.1126/science.aan0662

Haynes, B.F., Gilbert, P.B., McElrath, M.J., Zolla-Pazner, S., Tomaras, G.D., Alam, S.M., Evans, D.T., Montefiori, D.C., Karnasuta, C., Sutthent, R., Liao, H.-X., DeVico, A.L., Lewis, G.K., Williams, C., Pinter, A., Fong, Y., Janes, H., DeCamp, A., Huang, Y., Rao, M., Billings, E., Karasavvas, N., Robb, M.L., Ngauy, V., de Souza, M.S., Paris, R., Ferrari, G., Bailer, R.T., Soderberg, K.A., Andrews, C., Berman, P.W.,

650 Frahm, N., De Rosa, S.C., Alpert, M.D., Yates, N.L., Shen, X., Koup, R.A.,
651 Pitisuttithum, P., Kaewkungwal, J., Nitayaphan, S., Rerks-Ngarm, S., Michael, N.L.,
652 Kim, J.H., 2012. Immune-correlates analysis of an HIV-1 vaccine efficacy trial. N.
653 Engl. J. Med. 366, 1275–1286. doi:10.1056/NEJMoa1113425
654 Hessell, A.J., Hangartner, L., Hunter, M., Havenith, C.E.G., Beurskens, F.J., Bakker,
655 J.M., Lanigan, C.M.S., Landucci, G., Forthal, D.N., Parren, P.W.H.I., Marx, P.A.,
656 Burton, D.R., 2007. Fc receptor but not complement binding is important in antibody
657 protection against HIV. Nature 449, 101–104. doi:10.1038/nature06106
658 Hessell, A.J., Malherbe, D.C., Haigwood, N.L., 2018. Passive and active antibody
659 studies in primates to inform HIV vaccines. Expert Rev. Vaccines 17, 127–144.
660 doi:10.1080/14760584.2018.1425619
661 Hu, H., Eller, M.A., Zafar, S., Zhou, Y., Gu, M., Wei, Z., Currier, J.R., Marovich, M.A.,
662 Kibuuka, H.N., Bailer, R.T., Koup, R.A., Robb, M.L., Michael, N.L., Kim, J.H., Ratto-
663 Kim, S., 2014. Preferential infection of human Ad5-specific CD4 T cells by HIV in
664 Ad5 naturally exposed and recombinant Ad5-HIV vaccinated individuals. Proc. Natl.
665 Acad. Sci. U.S.A. 111, 13439–13444. doi:10.1073/pnas.1400446111
666 Huang, Y., Ferrari, G., Alter, G., Forthal, D.N., Kappes, J.C., Lewis, G.K., Love, J.C.,
667 Borate, B., Harris, L., Greene, K., Gao, H., Phan, T.B., Landucci, G., Goods, B.A.,
668 Dowell, K.G., Cheng, H.D., Bailey-Kellogg, C., Montefiori, D.C., Ackerman, M.E.,
669 2016. Diversity of Antiviral IgG Effector Activities Observed in HIV-Infected and
670 Vaccinated Subjects. The Journal of Immunology 197, 4603–4612.
671 doi:10.4049/jimmunol.1601197
672 Johansson, S.E., Rollman, E., Chung, A.W., Center, Rob J., Hejdeman, B., Stratov, I.,
673 Hinkula, J., Wahren, B., Kärre, K., Kent, S.J., Berg, L., 2011. NK cell function and
674 antibodies mediating ADCC in HIV-1-infected viremic and controller patients. Viral
675 Immunol. 24, 359–368. doi:10.1089/vim.2011.0025
676 Keele, B.F., Li, W., Borducchi, E.N., Nkolola, J.P., Abbink, P., Chen, B., Seaman, M.S.,
677 Barouch, D.H., 2017. Adenovirus prime, Env protein boost vaccine protects against
678 neutralization-resistant SIVsmE660 variants in rhesus monkeys. Nat. Commun. 8,
679 15740. doi:10.1038/ncomms15740
680 Kirmaier, A., Wu, F., Newman, R.M., Hall, L.R., Morgan, J.S., O'Connor, S., Marx, P.A.,
681 Meythaler, M., Goldstein, S., Buckler-White, A., Kaur, A., Hirsch, V.M., Johnson,
682 W.E., 2010. TRIM5 suppresses cross-species transmission of a primate
683 immunodeficiency virus and selects for emergence of resistant variants in the new
684 species. PLoS Biol. 8. doi:10.1371/journal.pbio.1000462
685 Klasse, P.J., Ketas, T.J., Cottrell, C.A., Ozorowski, G., Debnath, G., Camara, D.,
686 Francomano, E., Pugach, P., Ringe, R.P., LaBranche, C.C., van Gils, M.J., Bricault,
687 C.A., Barouch, D.H., Crotty, S., Silvestri, G., Kasturi, S., Pulendran, B., Wilson, I.A.,
688 Montefiori, D.C., Sanders, R.W., Ward, A.B., Moore, J.P., 2018. Epitopes for
689 neutralizing antibodies induced by HIV-1 envelope glycoprotein BG505 SOSIP
690 trimers in rabbits and macaques. PLoS Pathog. 14, e1006913.
691 doi:10.1371/journal.ppat.1006913
692 Krammer, F., Palese, P., 2015. Advances in the development of influenza virus
693 vaccines. Nat Rev Drug Discov 14, 167–182. doi:10.1038/nrd4529

694 Kristensen, A.B., Kent, S.J., Parsons, M.S., 2018. Contribution of NK cell education to
695 both direct and anti-HIV-1 antibody-dependent NK cell functions. J. Virol.
696 doi:10.1128/JVI.02146-17
697 Kulp, D.W., Steichen, J.M., Pauthner, M., Hu, X., Schiffner, T., Liguori, A., Cottrell, C.A.,
698 Havenar-Daughton, C., Ozorowski, G., Georgeson, E., Kalyuzhniy, O., Willis, J.R.,
699 Kubitz, M., Adachi, Y., Reiss, S.M., Shin, M., de Val, N., Ward, A.B., Crotty, S.,
700 Burton, D.R., Schief, W.R., 2017. Structure-based design of native-like HIV-1
701 envelope trimers to silence non-neutralizing epitopes and eliminate CD4 binding.
702 Nat. Commun. 8, 1655. doi:10.1038/s41467-017-01549-6
703 Laird Smith, M., Murrell, B., Eren, K., Ignacio, C., Landais, E., Weaver, S., Phung, P.,
704 Ludka, C., Hepler, L., Caballero, G., Pollner, T., Guo, Y., Richman, D., Poignard, P.,
705 Paxinos, E.E., Kosakovsky-Pond, S.L., Smith, D.M., 2016. Rapid Sequencing of
706 Complete env Genes from Primary HIV-1 Samples. Virus. Evol. 2, vew018.
707 doi:10.1093/ve/vew018
708 Li, H., Bar, K.J., Wang, S., Decker, J.M., Chen, Y., Sun, C., Salazar-Gonzalez, J.F.,
709 Salazar, M.G., Learn, G.H., Morgan, C.J., Schumacher, J.E., Hraber, P., Giorgi,
710 E.E., Bhattacharya, T., Korber, B.T., Perelson, A.S., Eron, J.J., Cohen, M.S., Hicks,
711 C.B., Haynes, B.F., Markowitz, M., Keele, B.F., Hahn, B.H., Shaw, G.M., 2010. High
712 Multiplicity Infection by HIV-1 in Men Who Have Sex with Men. PLoS Pathog. 6,
713 e1000890. doi:10.1371/journal.ppat.1000890
714 Li, H., Wang, S., Kong, R., Ding, W., Lee, F.-H., Parker, Z., Kim, E., Learn, G.H., Hahn,
715 P., Ben Policicchio, Brocca-Cofano, E., Deleage, C., Hao, X., Chuang, G.-Y.,
716 Gorman, J., Gardner, M., Lewis, M.G., Hatziioannou, T., Santra, S., Apetrei, C.,
717 Pandrea, I., Alam, S.M., Liao, H.-X., Shen, X., Tomaras, G.D., Farzan, M.,
718 Chertova, E., Keele, B.F., Estes, J.D., Lifson, J.D., Doms, R.W., Montefiori, D.C.,
719 Haynes, B.F., Sodroski, J.G., Kwong, P.D., Hahn, B.H., Shaw, G.M., 2016.
720 Envelope residue 375 substitutions in simian-human immunodeficiency viruses
721 enhance CD4 binding and replication in rhesus macaques. Proc. Natl. Acad. Sci.
722 U.S.A. 113, E3413–E3422. doi:10.1073/pnas.1606636113
723 Liu, J., Keele, B.F., Li, H., Keating, S., Norris, P.J., Carville, A., Mansfield, K.G.,
724 Tomaras, G.D., Haynes, B.F., Kolodkin-Gal, D., Letvin, N.L., Hahn, B.H., Shaw,
725 G.M., Barouch, D.H., 2010. Low-dose mucosal simian immunodeficiency virus
726 infection restricts early replication kinetics and transmitted virus variants in rhesus
727 monkeys. J. Virol. 84, 10406–10412. doi:10.1128/JVI.01155-10
728 Lovgren-Bengtsson, K., adjuvants, B.M.V., 2000, n.d. The ISCOMTM technology.
729 Humana Press Inc. Totowa.
730 Martins, M.A., Watkins, D.I., 2017. What Is the Predictive Value of Animal Models for
731 Vaccine Efficacy in Humans? Rigorous Simian Immunodeficiency Virus Vaccine
732 Trials Can Be Instructive. Cold Spring Harb. Perspect. Biol.
733 doi:10.1101/cshperspect.a029504
734 Mascola, J.R., Stiegler, G., VanCott, T.C., Katinger, H., Carpenter, C.B., Hanson, C.E.,
735 Beary, H., Hayes, D., Frankel, S.S., Birx, D.L., Lewis, M.G., 2000. Protection of
736 macaques against vaginal transmission of a pathogenic HIV-1/SIV chimeric virus by
737 passive infusion of neutralizing antibodies. Nat Med 6, 207–210. doi:10.1038/72318
738 Moldt, B., Rakasz, E.G., Schultz, N., Chan-Hui, P.-Y., Swiderek, K., Weisgrau, K.L.,
739 Piaskowski, S.M., Bergman, Z., Watkins, D.I., Poignard, P., Burton, D.R., 2012.

740 Highly potent HIV-specific antibody neutralization in vitro translates into effective
741 protection against mucosal SHIV challenge in vivo. Proc. Natl. Acad. Sci. U.S.A.
742 109, 18921–18925. doi:10.1073/pnas.1214785109
743 Pal, R., Wang, S., Kalyanaraman, V.S., Nair, B.C., Whitney, S., Keen, T., Hocker, L.,
744 Hudacik, L., Rose, N., Mboudjeka, I., Shen, S., Wu-Chou, T.-H., Montefiori, D.,
745 Mascola, J., Markham, P., Lu, S., 2006. Immunization of rhesus macaques with a
746 polyvalent DNA prime/protein boost human immunodeficiency virus type 1 vaccine
747 elicits protective antibody response against simian human immunodeficiency virus
748 of R5 phenotype. Virology 348, 341–353. doi:10.1016/j.virol.2005.12.029
749 Parren, P.W., Marx, P.A., Hessell, A.J., Luckay, A., Harouse, J., Cheng-Mayer, C.,
750 Moore, J.P., Burton, D.R., 2001. Antibody protects macaques against vaginal
751 challenge with a pathogenic R5 simian/human immunodeficiency virus at serum
752 levels giving complete neutralization in vitro. J. Virol. 75, 8340–8347.
753 doi:10.1128/JVI.75.17.8340-8347.2001
754 Pauthner, M., Havenar-Daughton, C., Sok, D., Nkolola, J.P., Bastidas, R., Boopathy,
755 A.V., Carnathan, D.G., Chandrashekar, A., Cirelli, K.M., Cottrell, C.A., Eroshkin,
756 A.M., Guenaga, J., Kaushik, K., Kulp, D.W., Liu, J., McCoy, L.E., Oom, A.L.,
757 Ozorowski, G., Post, K.W., Sharma, S.K., Steichen, J.M., de Taeye, S.W., Tokatlian,
758 T., Torrents de la Peña, A., Butera, S.T., LaBranche, C.C., Montefiori, D.C.,
759 Silvestri, G., Wilson, I.A., Irvine, D.J., Sanders, R.W., Schief, W.R., Ward, A.B.,
760 Wyatt, R.T., Barouch, D.H., Crotty, S., Burton, D.R., 2017. Elicitation of Robust Tier
761 2 Neutralizing Antibody Responses in Nonhuman Primates by HIV Envelope Trimer
762 Immunization Using Optimized Approaches. Immunity 46, 1073–1088.e6.
763 doi:10.1016/j.immuni.2017.05.007
764 Pegu, A., Yang, Z.-Y., Boyington, J.C., Wu, L., Ko, S.-Y., Schmidt, S.D., McKee, K.,
765 Kong, W.-P., Shi, W., Chen, X., Todd, J.-P., Letvin, N.L., Huang, J., Nason, M.C.,
766 Hoxie, J.A., Kwong, P.D., Connors, M., Rao, S.S., Mascola, J.R., Nabel, G.J., 2014.
767 Neutralizing antibodies to HIV-1 envelope protect more effectively in vivo than those
768 to the CD4 receptor. Sci. Transl. Med. 6, 243ra88–243ra88.
769 doi:10.1126/scitranslmed.3008992
770 Provine, N.M., Cortez, V., Chohan, V., Overbaugh, J., 2012. The neutralization
771 sensitivity of viruses representing human immunodeficiency virus type 1 variants of
772 diverse subtypes from early in infection is dependent on producer cell, as well as
773 characteristics of the specific antibody and envelope variant. Virology 427, 25–33.
774 doi:10.1016/j.virol.2012.02.001
775 Qureshi, H., Ma, Z.-M., Huang, Y., Hodge, G., Thomas, M.A., DiPasquale, J., DeSilva,
776 V., Fritts, L., Bett, A.J., Casimiro, D.R., Shiver, J.W., Robert-Guroff, M., Robertson,
777 M.N., McChesney, M.B., Gilbert, P.B., Miller, C.J., 2012. Low-dose penile
778 SIVmac251 exposure of rhesus macaques infected with adenovirus type 5 (Ad5)
779 and then immunized with a replication-defective Ad5-based SIV gag/pol/nef vaccine
780 recapitulates the results of the phase IIb step trial of a similar HIV-1 vaccine. J. Virol.
781 86, 2239–2250. doi:10.1128/JVI.06175-11
782 Reiss, S., Baxter, A.E., Cirelli, K.M., Dan, J.M., Morou, A., Daigneault, A., Brassard, N.,
783 Silvestri, G., Routy, J.P., Havenar-Daughton, C., Crotty, S., Kaufmann, D.E., 2017.
784 Comparative analysis of activation induced marker (AIM) assays for sensitive

identification of antigen-specific CD4 T cells. PLoS ONE 12, e0186998. doi:10.1371/journal.pone.0186998

Richard, J., Prévost, J., Baxter, A.E., Bredow, von, B., Ding, S., Medjahed, H., Delgado, G.G., Brassard, N., Stürzel, C.M., Kirchhoff, F., Hahn, B.H., Parsons, M.S., Kaufmann, D.E., Evans, D.T., Finzi, A., 2018. Uninfected Bystander Cells Impact the Measurement of HIV-Specific Antibody-Dependent Cellular Cytotoxicity Responses. mBio 9, e00358–18. doi:10.1128/mBio.00358-18

Roederer, M., Keele, B.F., Schmidt, S.D., Mason, R.D., Welles, H.C., Fischer, W., Labranche, C., Foulds, K.E., Louder, M.K., Yang, Z.-Y., Todd, J.-P.M., Buzby, A.P., Mach, L.V., Shen, L., Seaton, K.E., Ward, B.M., Bailer, R.T., Gottardo, R., Gu, W., Ferrari, G., Alam, S.M., Denny, T.N., Montefiori, D.C., Tomaras, G.D., Korber, B.T., Nason, M.C., Seder, R.A., Koup, R.A., Letvin, N.L., Rao, S.S., Nabel, G.J., Mascola, J.R., 2015. Immunological and virologicalmechanisms of vaccine-mediatedprotection against SIV and HIV. Nature 505, 502–508. doi:10.1038/nature12893

Sanders, R.W., Derking, R., Cupo, A., Julien, J.-P., Yasmeen, A., de Val, N., Kim, H.J., Blattner, C., la Peña, de, A.T., Korzun, J., Golabek, M., de Los Reyes, K., Ketas, T.J., van Gils, M.J., King, C.R., Wilson, I.A., Ward, A.B., Klasse, P.J., Moore, J.P., 2013. A next-generation cleaved, soluble HIV-1 Env trimer, BG505 SOSIP.664 gp140, expresses multiple epitopes for broadly neutralizing but not non-neutralizing antibodies. PLoS Pathog. 9, e1003618–e1003618. doi:10.1371/journal.ppat.1003618

Sanders, R.W., van Gils, M.J., Derking, R., Sok, D., Ketas, T.J., Burger, J.A., Ozorowski, G., Cupo, A., Simonich, C., Goo, L., Arendt, H., Kim, H.J., Lee, J.H., Pugach, P., Williams, M., Debnath, G., Moldt, B., van Breemen, M.J., Isik, G., Medina-Ramírez, M., Back, J.W., Koff, W.C., Julien, J.-P., Rakasz, E.G., Seaman, M.S., Guttman, M., Lee, K.K., Klasse, P.J., Labranche, C., Schief, W.R., Wilson, I.A., Overbaugh, J., Burton, D.R., Ward, A.B., Montefiori, D.C., Dean, H., Moore, J.P., 2015. HIV-1 neutralizing antibodies induced by native-like envelope trimers. Science 349, aac4223–aac4223. doi:10.1126/science.aac4223

Shingai, M., Donau, O.K., Plishka, R.J., Buckler-White, A., Mascola, J.R., Nabel, G.J., Nason, M.C., Montefiori, D., Moldt, B., Poignard, P., Diskin, R., Bjorkman, P.J., Eckhaus, M.A., Klein, F., Mouquet, H., Cetrulo Lorenzi, J.C., Gazumyan, A., Burton, D.R., Nussenzweig, M.C., Martin, M.A., Nishimura, Y., 2014. Passive transfer of modest titers of potent and broadly neutralizing anti-HIV monoclonal antibodies block SHIV infection in macaques. Journal of Experimental Medicine 211, 2061–2074. doi:10.1084/jem.20132494

Sok, D., Le, K.M., Vadnais, M., Saye-Francisco, K.L., Jardine, J.G., Torres, J.L., Berndsen, Z.T., Kong, L., Stanfield, R., Ruiz, J., Ramos, A., Liang, C.-H., Chen, P.L., Criscitiello, M.F., Mwangi, W., Wilson, I.A., Ward, A.B., Smider, V.V., Burton, D.R., 2017. Rapid elicitation of broadly neutralizing antibodies to HIV by immunization in cows. Nature 548, 108–111. doi:10.1038/nature23301

Staprans, S.I., Barry, A.P., Silvestri, G., Safrit, J.T., Kozyr, N., Sumpter, B., Nguyen, H., McClure, H., Montefiori, D., Cohen, J.I., Feinberg, M.B., 2004. Enhanced SIV replication and accelerated progression to AIDS in macaques primed to mount a

CD4 T cell response to the SIV envelope protein. Proc. Natl. Acad. Sci. U.S.A. 101, 13026–13031. doi:10.1073/pnas.0404739101

Stephenson, K.E., D'Couto, H.T., Barouch, D.H., 2016. New concepts in HIV-1 vaccine development. Curr. Opin. Immunol. 41, 39–46. doi:10.1016/j.coi.2016.05.011

Sundling, C., Martinez, P., Soldemo, M., Spångberg, M., Bengtsson, K.L., Stertman, L., Forsell, M.N.E., Hedestam, G.B.K., 2013. Immunization of macaques with soluble HIV type 1 and influenza virus envelope glycoproteins results in a similarly rapid contraction of peripheral B-cell responses after boosting. Journal of Infectious Diseases 207, 426–431. doi:10.1093/infdis/jis696

Tomaras, G.D., Plotkin, S.A., 2017. Complex immune correlates of protection in HIV-1 vaccine efficacy trials. Immunol. Rev. 275, 245–261. doi:10.1111/imr.12514

Torrents de la Peña, A., de Taeye, S.W., Sliepen, K., LaBranche, C.C., Burger, J.A., Schermer, E.E., Montefiori, D.C., Moore, J.P., Klasse, P.J., Sanders, R.W., 2018. Immunogenicity in rabbits of SOSIP trimers from clades A, B and C, given individually, sequentially or in combinations. J. Virol. 92. doi:10.1128/JVI.01957-17

Torrents de la Peña, A., Julien, J.-P., de Taeye, S.W., Garces, F., Guttman, M., Ozorowski, G., Pritchard, L.K., Behrens, A.-J., Go, E.P., Burger, J.A., Schermer, E.E., Sliepen, K., Ketas, T.J., Pugach, P., Yasmeen, A., Cottrell, C.A., Torres, J.L., Vavourakis, C.D., van Gils, M.J., Labranche, C., Montefiori, D.C., Desaire, H., Crispin, M., Klasse, P.J., Lee, K.K., Moore, J.P., Ward, A.B., Wilson, I.A., Sanders, R.W., 2017. Improving the Immunogenicity of Native-like HIV-1 Envelope Trimers by Hyperstabilization. Cell Rep 20, 1805–1817. doi:10.1016/j.celrep.2017.07.077

Veillette, M., Coutu, M., Richard, J., Batraville, L.-A., Dagher, O., Bernard, N., Tremblay, C., Kaufmann, D.E., Roger, M., Finzi, A., 2015. The HIV-1 gp120 CD4-bound conformation is preferentially targeted by antibody-dependent cellular cytotoxicity-mediating antibodies in sera from HIV-1-infected individuals. J. Virol. 89, 545–551. doi:10.1128/JVI.02868-14

Veillette, M., Coutu, M., Richard, J., Batraville, L.-A., Désormeaux, A., Roger, M., Finzi, A., 2014. Conformational Evaluation of HIV-1 Trimeric Envelope Glycoproteins Using a Cell-based ELISA Assay. JoVE 1–8. doi:10.3791/51995

STAR METHODS

CONTACT FOR REAGENT AND RESOURCE SHARING

Further information and requests for resources and reagents should be directed to and will be fulfilled by Dennis Burton (burton@scripps.edu).

EXPERIMENTAL MODEL AND SUBJECT DETAILS

Rhesus macaques

Outbred Indian rhesus macaques (*Macaca mulatta*) were sourced and housed at Alphagenesis Inc, Yemasee, SC and maintained in accordance with NIH guidelines. These studies were approved by the appropriate Institutional Animal Care and Use Committees (IACUC). None of the NHPs were previously enrolled in other studies that are not explicity stated in the manuscript. All animals were genotyped for class I alleles Mamu-A*01, Mamu-B*08 and Mamu-B*17 and Trim5, which are associated with spontaneous virological control. Genotype and gender information for all animals is reported in Table S1. Additional information on high- and low-nAb titer group animals is published in Pauthner et al., 2017.

METHOD DETAILS

Rhesus monkey immunizations and challenge

Animals were immunized at 4 weeks before challenge (week -4) with a fourth dose of the previously administered immunogen for a given animal with adjuvant (Figure S1B)

883 (Pauthner et al., 2017). The adjuvant used for this boost was an ISCOMATRIX-like
884 nanoparticle comprised of self-assembled cholesterol, phospholipid, and Quillaja saponin
885 prepared as previously described (Lovgren-Bengtsson et al., n.d.). All immunizations
886 were administered as split doses. Each immunization consisted of two subcutaneous
887 injections of 50 µg of Env trimer protein + 187.5 units (U) of saponin adjuvant, in sterile
888 phosphate-buffered saline (PBS) diluent for a total of 100 µg of Env trimer protein + 375
889 U of Iscomatrix per immunization per animal. Subcutaneous immunizations were given in
890 a volume of 0.5 ml with a 1 inch, 25-gauge needle at the medial inner mid-thigh of each
891 leg. The subcutaneous injection technique consists of making a 'skin tent' and inserting
892 the needle into the subcutaneous space at a 45˚angle.

893 Serum was collected in SST Vaccutainer tubes (BD Biosciences) and processed
894 according to the manufacturer's instructions. Multiple aliquots of 0.5 ml were frozen at
895 -80° C. Whole blood was collected in K2 EDTA Vaccutainer tubes (BD Biosciences) for
896 plasma and PBMC isolation. Multiple aliquots of 0.5 ml of plasma were frozen at -80° C.
897 PBMCs were isolated using Thermo Scientific Nunc EZFlip Conical Centrifuge Tubes per
898 manufacturer's instructions. PBMCs were isolated, counted, and re-suspended at 1 x 10^7
899 cells/mL in FBS containing 10% DMSO. Aliquots were subsequently frozen in 1 mL vials
900 using a Mr. Frosty freezing container (Nalgene, cooling rate of 1°C / minute) and placed
901 in a -80° C freezer. The following day PBMC samples were moved to storage in a liquid
902 nitrogen freezer tank.

903 Animals were atraumatically inoculated intrarectally with a 1:75 dilution of rhCD4-
904 grown SHIVBG505 N332 S375Y ΔCT challenge stock (Li et al., 2016) in RPMI 1640
905 (Gibco), which amounted to 1.4 *10^7 virions or 2 ng p27. See dataset S1B in Li et al. (Li

et al., 2016) for a complete characterization of the challenge stock with respect to virion content and virion infectivity.

Viral Load Assay

Plasma SHIV RNA levels in serum following infection were measured using a *gag*-targeted quantitative real-time RT-PCR assay as previously described (Hansen et al., 2013).

Serum neutralization assays

Replication incompetent HIV pseudovirus was produced by co-transfecting *env* plasmids with an *env*-deficient backbone plasmid (pSG3Δ*env*) in HEK293T cells in a 1:2 ratio, using the X-tremeGENE 9 transfection reagent (Roche). Pseudovirus was harvested after 48-72 h by sterile-filtration (0.22 μm) of cell culture supernatants, and neutralization was tested by incubating pseudovirus and serum or mAbs for 1 h at 37 °C before transferring them onto TZM-bl cells as previously described (Pauthner et al., 2017). For replication competent $SHIV_{BG505}$ neutralization, rhCD4-grown $SHIV_{BG505}$ N332 S375Y challenge stock was used instead in a BSL3 facility with no further modifications.

Neutralization is measured in duplicate wells within each experiment. BG505 nAb titers for group comparisons were measured in three or more independent experiments that were subsequently averaged. The BG505 pseudovirus time course neutralization data shown in Figure 3 were generated in single large experiments, to test sera from all time points side-by-side, thus ensuring the highest nAb titer comparability between time

928 points. Neutralization was tested starting at 1:10 serum dilutions followed by nine serial
929 3-fold dilutions to ensure the highest sensitivity and range of detection. Neutralization ID_{50}
930 titers were calculated using the 'One site – Fit logIC_{50}' regression in Graphpad Prism v7.0.
931 ID_{50} nAb titers of incomplete neutralization curves that reached at least 50%, but less than
932 90% maximal neutralization, were calculated by constraining the regression fit through
933 0% and 100% neutralization, to ensure accurate calculation of half-way (50%) nAb titers.
934 All neutralization titers are reported as ID_{50} titers. All nAb titer data panels show geometric
935 mean titers with geometric SD. BG505 pseudovirus neutralization was tested using the
936 BG505.W6M.ENV.C2 isolate (AIDS Reagents Program), carrying the T332N mutation to
937 restore the N332 glycosylation site, as well as other indicated mutations that were added
938 by site-directed mutagenesis.

939

940 **Serum binding ELISAs**

941 Microlon 96-well plates (Corning) were coated overnight with streptavidin at 2.5 µg/mL
942 (Thermo Scientific). Plates were then washed 4-5 times with PBS-tween (0.05%) and
943 blocked with PBS + 3% BSA for 1 h at room temperature. If capturing biotinylated BG505
944 SOSIP.664-Avi or BG505-Avi gp120, proteins were added at 2.5 µg/mL in PBS + 1% BSA
945 for 2 h at room temperature. For V3-peptide binding assays, no streptavidin was coated
946 and instead BG505 V3-peptide (TRPNNNTRKSIRIGPGQAFYATG) was directly coated
947 to Microlon 96-well plates at 2.5 µg/mL in PBS overnight. Plates were then washed 4-5
948 times with PBS-tween (0.05%) and serially diluted sera in PBS + 1% BSA were then
949 added for 1 h at room temperature. Plates were then washed 4-5 times with PBS-tween
950 (0.05%) and alkaline phosphatase-conjugated goat anti-human IgG (Jackson

ImmunoResearch) was added for 1 h at a 1:1000 dilution (final concentration 0.33 µg/mL) in PBS + 1% BSA at room temperature. Plates were then washed 4-5 times with PBS-tween (0.05%) and absorption at 405 nm was measured following addition of phosphatase substrate in alkaline phosphatase buffer. We calculated half maximal EC_{50} binding titers using Graphpad Prism v7.0. All ELISA Ab data panels show geometric mean titers with geometric SD.

ADCC assays

Luciferase-based CEM.NKR SHIV, HIV, SIV infection assay

ADCC activity was measured as previously described (Alpert et al., 2012). CEM.NKR-$_{CCR5}$-sLTR-Luc cells, which express luciferase (Luc) upon infection, were infected with either HIV-1 BG505, SHIV BG505 or $SIV_{mac}239$ by spinoculation in the presence of 40 µg/ml of polybrene. For HIV-1 BG505 and $SHIV_{BG505}$ infections, *vif*-deleted infectious molecular clones were pseudotyped with Vesicular stomatitis virus G (VSVG). Two days post-infection with VSVG-pseudotyped HIV-1/$SHIV_{BG505}$ and 4 days post-infection with $SIV_{mac}239$, CEM.NKR-$_{CCR5}$-sLTR-Luc cells were incubated at a 10:1 effector:target cell ratio either with an NK cell line expressing rhesus macaque CD16 in the presence of serial dilutions of rhesus macaque sera or an NK cell line expressing human CD16 in the presence of human monoclonal bnAbs. After an 8-hour incubation, Luc activity was measured using BriteLite luciferase substrate (PerkinElmer). Uninfected or infected cells incubated with NK cells in the absence of antibody or plasma were used to determine background and maximal Luc activity, respectively. The dose-dependent loss of Luc activity represents the antibody-dependent killing of productively infected target cells.

974

975 *FACS-based CEM.NKR SHIV infection assay*

976 VSVG-pseudotyped $SHIV_{BG505}$ N332 S375Y virus was produced and titrated as
977 previously described (Veillette et al., 2015). Viruses were then used to infect CEM.NKR-
978 $CCR5$-sLTR-Luc cells by spin infection at 800 × *g* for 1 h in 96-well plates at 25 °C.
979 Measurement of ADCC using the FACS-based assay was performed at 48h post-infection
980 as previously described (Veillette et al., 2015). Briefly, infected CEM.NKR-$_{CCR5}$-sLTR-
981 Luc cells were stained with viability (AquaVivid; Thermo Fisher Scientific) and cellular (cell
982 proliferation dye eFluor670; eBioscience) markers and used as target cells. Human
983 PBMCs isolated from three different healthy HIV-uninfected individuals were used as
984 effector cells and were stained with another cellular marker (cell proliferation dye
985 eFluor450; eBioscience). Effector cells were added at an effector:target cell ratio of 10:1
986 in 96-well V-bottom plates (Corning, Corning, NY). A 1:250 final dilution of sera or 5 μg/ml
987 of mAbs were added to appropriate wells and cells were incubated for 15 min at room
988 temperature. The plates were subsequently centrifuged for 1 min at 300 g, and incubated
989 at 37°C, 5% CO_2 for 5 to 6 h before being fixed with a PBS-formaldehyde solution (2%
990 formaldehyde final concentration). Cells were then permeabilized using the
991 Cytofix/Cytoperm Fixation/Permeabilization Kit (BD Biosciences) and SHIV-infected cells
992 were identified by intracellular staining using Alexa fluor 488-conjugated anti-p27 Abs
993 (clone 2F12). Samples were analyzed on an LSRII cytometer (BD Biosciences). Data
994 analysis was performed using FlowJo vX.0.7 (Tree Star). The percentage of ADCC was
995 calculated with the following formula: (% of p27+ cells in Targets plus Effectors) − (% of
996 p27+ cells in Targets plus Effectors plus Abs or sera) / (% of p27+ cells in Targets) by

997 gating on infected living target cells. Of note, samples were deidentified and tested and
998 analyzed blindly.

999

1000 *FACS-based gp120-coated CEM.NKR ADCC assay*

1001 CEM.NKR-$_{CCR5}$-sLTR-Luc cells were coated with 1µg of recombinant HIV-1$_{BG505}$ N332
1002 gp120/million cells for 30 min at 37°C. gp120-coated target cells were used as target cells
1003 and were stained with viability (AquaVivid; Thermo Fisher Scientific) and cellular (cell
1004 proliferation dye eFluor670; eBioscience) markers. ADCC was performed as described
1005 above with the difference that after target/effector cells co-incubation, cells were fixed
1006 with a PBS-formaldehyde solution (2% formaldehyde final concentration) containing a
1007 constant number of flow cytometry particles (5x10^4/ml) (AccuCount Blank Particles, 5.3
1008 µm; Spherotech, Lake Forest, IL, USA). These particles are designed to be used as
1009 reference particles since their concentration is known, thus allowing to count the absolute
1010 cell number by flow cytometry. A constant number of particles (1x10^3) were counted
1011 during cytometry acquisition in order to normalize the number of viable targets cells. Each
1012 sample was acquired with a LSRII (BD Bioscience, Mississauga, ON, Canada) and data
1013 analysis was performed using FlowJo vX.0.6 (Tree Star, Ashland, OR, USA). The
1014 percentage of ADCC was calculated with the following formula: (relative count of gp120-
1015 coated cells in targets plus effectors) - (relative count of gp120-coated cells in targets plus
1016 effectors plus Abs or sera) / (relative count of gp120-coated cells in targets) by gating live
1017 target cells (Veillette et al., 2015). Of note, samples were deidentified and tested and
1018 analyzed blindly.

1019

T cell analysis

Frozen aliquots of macaque PBMCs were thawed, washed once with RPMI + 10% FBS (R10), incubated with DNase (100ug/ml, StemCell Technologies 07900) for 15 minutes at 37C, then washed again and split in half for a $CD8^+$ ICS assay and a $CD4^+$ T cell Activation Induced Marker (AIM) assay (Reiss et al., 2017).

For the CD8+ T cell ICS assay, the sample was further split into three groups and either left unstimulated (NS), stimulated with BG505 Env peptides (5ug/ml), or stimulated with SEB (1ug/ml) for 2 hours at 37C. Brefeldin A was then added (2ug/ml), and the stimulations incubated for another 4 hours at 37C. The cells were then stained for 30 minutes at 4C with the fluorescent antibodies in the Surface Marker Panel below and washed twice with FACS buffer. They were fixed with eBio intranuclear fix/perm kit for 20 minutes, washed once with perm buffer, then stained with the antibodies in the Intranuclear Panel in perm buffer for 30 minutes at 4C. The samples were then washed with FACS buffer and acquired on a BD LSR Fortessa.

For the $CD4^+$ T cell AIM assay, the sample was further split into three groups and either left unstimulated (NS) or stimulated with BG505 Env peptides (5ug/ml), or stimulated with SEB (100 pg/ml) for 24 hours at 37C. The cells were then stained for 60 minutes at 4C with the fluorescent antibodies in the AIM Surface Marker Panel below, washed with FACS buffer, fixed with 1% formaldehyde for 10 minutes at 4C, then washed again before acquisition on a BD LSR Fortessa.

CD8 Surface Marker Panel:			
	CD4 (Clone SK3)	PerCP	1:200
	CD20 (Clone 2H7)	BV570	1:200
	CD8 (Clone RPA-T8)	BV650	1:200
	CCR5 (3A9)	APC	1:200
	a4b7 (Act-1)	PE	1:200
	Live/Dead	APC e780	1:1000
CD8 Intranuclear Panel:			
	Ki67 (B56)	Ax488	1:100
	IL2 (MQ1-17H12)	Ax700	1:100
	IFN (Clone B27)	Pac Blue	1:100
	TNF (MAb11)	PECy7	1:100
	CD40L (24-31)	BV605	1:100
CD4 T Cell AIM Surface Marker Panel:			
	CD4 (Clone OKT-4)	BV650	1:100
	CD20 (Clone 2H7)	BV570	1:100
	PD1 (Clone EH12.2H7)	BV785	1:100
	CXCR5 (Clone MU5UBEE)	PECy7	1:100
	Live/Dead	APC e780	1:1000
	CD14 (61D3)	APC e780	1:100
	CD16 (eBioCD16)	APC e780	1:100
	CD25 (Clone BC96)	FITC	1:100
	Ox40 (Clone L106)	PE	1:100
	4-1-BB (4B4-1)	BV421	1:100
	ICOS (C398.4A)	PerCP Cy5.5	1:100
	CXCR3 (1C6)	APC	1:100

Full length *env* viral sequencing

Long-read env sequencing

Samples were processed using the full-length Env sequencing protocol developed in (Laird Smith et al., 2016), but with modified primers and PCR conditions. Briefly, plasma samples were pelleted through a sucrose cushion to enrich for virions, RNA was extracted using the QIAamp Viral RNA Mini Kit (part no. 52906; Qiagen, Valencia, CA), and cDNA generated using the SuperScript III First Strand Synthesis System for RT-PCR (part no. 18080-051; Thermo Fisher, Fremont, CA), with oligo (dT) primers. SHIV *env* was amplified from this cDNA using the HIV *env* forward primer from (Laird Smith et al., 2016) Env-F: GAGCAGAAGACAGTGGCAATGA, and using a reverse primer designed for this SHIV: CCCTGATTGTATTTCTGTCCCTCAC, both purchased (de-salted) from Integrated DNA Technologies (San Diego, CA) and diluted to 20 pmol in 0.1X TE buffer before use. PCR was as in (Laird Smith et al., 2016), using the Advantage 2 PCR reaction mixture (Advantage 2 PCR Kit, catalog no. 639206; Clontech, Mountain View, CA), with the SA Buffer, but using 42 cycles of 15 sec denaturation at 95°C, 30 sec annealing at 64^{0}C, and 3 min extension at 68°C. A QIAquick PCR Purification Kit (part no. 28106; Qiagen, Valencia, CA) was used to purify PCR products, and Pacific Biosciences library preparation was exactly as in (Laird Smith et al., 2016), but using the newer P6/C4 chemistry, and with a modified 0.025nM loading concentration, and a 6 hour movie time. The challenge stock was handled identically but was highly concentrated and thus only 23 PCR cycles were used during amplification.

PacBio env data processing

An updated version of the Full-Length Env Analyzer (Eren et al., 2017; Laird Smith et al., 2016) pipeline was used to process SIV PacBio reads. Briefly, PacBio's CCS2 algorithm was used to reconstruct single molecule Circular Consensus Sequence (CCS) reads, outputting fastq files. These reads were filtered for length, quality, and for matching an Env reference database (here we included the known BG505.SHIV challenge sequence) with FLEA's default parameter settings. FLEA's error correction and data-summarizing approach was used, again with default parameters, collapsing near-identical reads and generating high-quality consensus sequences (HQCSs), along with HQCS frequencies, which are then codon aligned. These HQCS sequences are visualized in a web browser environment, allowing the exploration of immunotype frequencies, and displaying variants upon the leaf nodes of a maximum likelihood phylogeny. Variant frequencies in Figure S3A-B were computed from HQCS sequence frequencies.

Complex preparation for negative-stain EM

Serum Fab preparation was carried out as previously described (Bianchi et al., 2018). In brief, after buffer exchanging into TBS, up to ~1 mg of total Fab was incubated overnight with 10-15 µg BG505 trimers at RT in ~50 µL total volume. Complexes were then purified via size exclusion chromatography (SEC) using Superose 6 Increase 10/300 column (GE Healthcare) in order to remove unbound Fab. The flow-through fractions containing the complexes were pooled and concentrated using 100 kDa cutoff centrifugal filters (EMD Millipore). The final trimer concentration was titrated to 0.04 mg/mL prior to application onto carbon-coated copper grids.

Negative-stain EM

The SEC-purified complexes were applied to glow-discharged, carbon-coated 400-mesh copper grids, followed by pipetting 3 µl of 2% (w/v) uranyl formate stain and blotting, followed by application of another 3 µl of stain for 45–60 s, again followed by blotting. Stained grids were stored under ambient conditions until ready for imaging. Images were collected via Leginon software using a Tecnai T12 electron microscopes operated at 120 kV ×52,000 magnification. In all cases, the electron dose was 25 e−/A2. Particles were picked from the raw images using DoG Picker and placed into stacks using Appion software. 2D reference-free alignment was performed using iterative MSA/MRA. The particle stacks were then converted from IMAGIC to RELION-formatted MRC stacks and subjected to RELION 2.1 2D and 3D classification. A detailed protocol can be found in Bianchi et al., Immunity 2018.

QUANTIFICATION AND STATISTICAL ANALYSIS

Infection probability per challenge event was modeled as depending on the BG505 N332 S375Y log10 ID_{50} nAb titer at the time of challenge using a modified logistic regression, where the maximum infection probability (where $0 < max < 1$) was an additional parameter to be estimated by the model, rather than being fixed at 1 as in traditional logistic regression:

$$\frac{max}{1 + e^{-slope\ (x-offset)}}$$

This adjustment is necessary because unimmunized animals with no serum nAb titers are not infected with 100% probability upon the first challenge, as a consequence of the chosen AID_{75} challenge dose. The infection event was assumed to be the challenge time point prior to the detection of viremia. Per-time point challenge outcomes were assumed to be conditionally independent of each other when conditioning on the corresponding BG505 N332 S375Y log10 ID_{50} nAb titer of the respective time point. We assumed weakly informative priors over the three model parameters, with slope~*Normal*(0,10), offset~*Normal*(0,10), and max~*Uniform*(0,1), and we used the Metropolis algorithm to draw 1 million samples from the posterior distribution. Chain mixing was rapid (see trace plots in Figure S5B), with effective sample sizes (ESSs) above 20,000 for all 3 parameters and for the log posterior probability. The posterior parameter distributions are visualized in Figure S5A. The calculated 5%, 50%, and 95% quantiles for each parameter were:

slope: -6.32937, -3.49356, -1.99455

offset: 1.71374, 2.12005, 2.4339

max: 0.602868, 0.80477, 0.962382

While under the prior distribution, P(slope < 0) = 0.5 and P(slope > 0) = 0.5, allowing equal prior probability of protective or sensitizing effects of neutralizing antibodies, the posterior probability of P(slope < 0) = 1 indicated the strongest possible evidence for decreasing infection probabilities given increasing ID_{50} nAb titers. Figure S5C shows

10,000 posterior sampled logistic curves, and the 5%, median, and 95% credible intervals for the infection probability computed from these, that were used to plot Figure 4C.

Graphpad Prism v7.0 was used for all standard statistical analyses. The significance of differences in neutralization and binding data between groups was calculated using unpaired, two-tailed Mann-Whitney U tests, correlations were calculated using Spearman correlation tests. Statistical parameters of all analyses are reported in the respective figure legends.

KEY RESOURCES TABLE